Deep into the Chibougamau area, Abitibi greenstone belt: structure of a Neoarchean crust revealed by seismic reflection profiling

Lucie Mathieu[1], David B. Snyder[2], Pierre Bedeaux[1], Saeid Cheraghi[2], Bruno Lafrance[2], Phil Thurston[2], and Ross Sherlock[2]

[1]Centre d'études sur les ressources minérales (CERM), Département des Sciences appliquées, Université du Québec à Chicoutimi (UQAC), Chicoutimi, Québec

[2]Harquail School of Earth Science, Mineral Exploration Research Centre, Laurentian University, Sudbury, Ontario

Corresponding author: Lucie Mathieu (lucie1.mathieu@uqac.ca)

Key Points

- Seismic reflection survey of the Chibougamau area, northeastern corner of the Abitibi greenstone belt, by the Metal Earth project.
- The Metal Earth and Lithoprobe seismic surveys reveal that the northern part of the Abitibi greenstone belt has a consistent architecture.
- The Chibougamau area is an Archean oceanic crust evolved through terrane imbrication and not through plume activity and subduction processes.

Abstract

Copper-Au magmatic-hydrothermal systems dominate in the Chibougamau area of the Neoarchean Abitibi subprovince (greenstone belt) of the Superior Province (craton), whereas orogenic gold mineralization is more common in the rest of the Abitibi. Understanding differences in metal endowment within the Abitibi greenstone belt requires insights into the geodynamic evolution of the Chibougamau area. This was addressed by imaging the crust using seismic reflection profiling acquired as part of the Metal Earth project. Seismic reflection sections display shallowly south-dipping reflectors located within the upper-crust (e.g., deep continuation of the Barlow fault) and a northward-dipping mid-crust imbricated with older crust (Opatica subprovince) to the north. Multiple reflectors characterize the upper part of the mid-crust, interpreted as faults superimposed on a major lithological boundary. These structures likely formed during terrane accretion prior to craton stabilization. Combining the new seismic data with known stratigraphic, structural and magmatic records, we propose that the study area was initially a normal (i.e., thick) Archean oceanic crust that formed at or before 2.80 Ga and that evolved through terrane imbrication at 2.73-2.70 Ga. Shortening caused rapid burial, devolatilization and partial melting of hydrated mafic rocks to produce tonalite magmas that may have mixed with mantle-derived melts to produce the diorite-tonalite suite associated with observed Cu-Au magmatic-hydrothermal mineralization.

Keywords: Metal Earth project, seismic reflection, Chibougamau area, magmatic evolution, geodynamic processes, mineralization

1 Introduction

Archean greenstone belts host many of the world's major mineral resources, yet their crustal architecture and tectonic history are only partly understood. In addition, belts with comparable surface geology, e.g., Abitibi-Wawa and Wabigoon subprovinces (greenstone belts) in Canada, have significant differences in their metal endowment. Given the similar geology at surface, the geophysical investigation documented herein is crucial in understanding the architecture of the crust and to correlate metal endowment differences of terranes with crustal-scale features.

The Chibougamau area is located in the north-eastern corner of the Neoarchean Abitibi greenstone belt, in the southern part of the Superior Province (craton). Unlike other parts of the Abitibi greenstone belt, it is a Cu dominated belt with lesser Au endowment and was therefore chosen as a key area to investigate lithospheric controls on metal endowment of the Abitibi greenstone belt.

The Chibougamau area occupies the easternmost part of the 430 km long, E-W-striking Matagami-Chibougamau greenstone belt. The eastern part of this belt has not previously been imaged by deep seismic reflection methods and, as most Neoarchean terranes, its geodynamic evolution is controversial. The Chibougamau area had a crustal evolution that led to magmatism favorable to magmatic-hydrothermal mineralizing processes and formation of the large Central Camp Cu-Au porphyry system (P Pilote et al., 1997). Magmatic-hydrothermal mineralization is rare in the Abitibi greenstone belt better known for its orogenic gold and VMS (volcanogenic massive sulfide) ore systems (Dubé & Gosselin, 2007; Gosselin & Dubé, 2005). Chibougamau also lacks terrane-bounding fault zones such as the Cadillac-Larder Lake fault of southern Abitibi (Bedeaux et al., 2018; Poulsen, 2017). This contribution focuses on the geodynamic evolution and economic potential of the Chibougamau area, which are unraveled using new seismic reflection data combined with the current stratigraphic, structural and magmatic observations and interpretations for the area.

Seismic reflection profiling methods provide the highest resolution image of crustal architecture at depths greater than a few kilometers (Sheriff & Geldart, 1995). Such data provide insights into, for example, lithological contacts, fault zones, altered areas (Eaton, 2006) and can provide invaluable insights into the architecture and geodynamic evolution of the crust. Similar regional seismic transects across the Superior craton were done ~30 years ago as part of the Lithoprobe program (Calvert & Ludden, 1999; Percival & West, 1994; White et al., 2003). Lithoprobe's main goal was to image the crust and crust-mantle boundary. Its regional transects emphasized deep signal penetration, resulting in low resolution of near-surface reflectors. The more recent Discovery Abitibi seismic surveys obtained better near-surface resolution but were restricted to a few areas (Ayer et al., 2008; Snyder et al., 2008). The Chibougamau seismic transect is one of 13 transects under the Metal Earth program (2017-2023), which also emphasizes near-surface resolution. Combined with surface geology data, the new Metal Earth seismic profile provides fresh insights into the structure of the Chibougamau area, its geodynamic evolution and its mineralizing systems.

2 Geological Setting

The thickest package of rocks in the Chibougamau area belongs to the ca. >2730 Ma to 2710 Ma Roy Group, which sits on ca. 2790-2760 Ma volcanic units (Chrissie and Des Vents formations) and is overlain by the sedimentary units of the Opémisca Group (**Figure 1**). The Roy Group is divided into volcanic cycle 1, which consists of mafic to intermediate lava flows, and volcanic cycle 2, which consists of mafic flows overlain by intermediate to felsic flows and fragmental units (Leclerc et al., 2017). In this contribution, the magmatic events that formed the Roy Group and its coeval plutons, as well as older volcanic rocks, will be referred to as the synvolcanic period, while later events that led to craton stabilization will receive the general designation 'syntectonic period'. Rocks exposed in the Chibougamau area were metamorphosed to greenschist facies grade, as have most rocks of the Abitibi greenstone belt (Faure, 2015; Jolly, 1974). To simplify the text, the prefix "meta-" is omitted from the rock names.

2.1 Stratigraphy and volcanic environment

The oldest volcanic rocks of the Chibougamau area are mafic and felsic lava flows and volcanoclastic deposits of the Chrissie and Des Vents formations, which crop out 2 to 10 km west of the seismic profile (**Table 1**). These rocks predate the deposition of the 7-14 km thick Roy Group and Opémisca Group (Mueller et al., 1989).

Volcanic cycle 1 of the Roy Group consists mainly of mafic to intermediate lava flows of the Obatogamau Formation (R. Daigneault & Allard, 1990; Mueller et al., 1989) overlain by sulphide-bearing intermediate to felsic, coherent (e.g., lava dome) to clastic (pyroclastic to sedimentary units) volcanic rocks of the Waconichi Formation (Caty, 1975). The mostly effusive volcanic cycle 1 is thought to represent submarine lava plains topped by small volcanic centers (Mueller et al., 1989), which formed in submarine valleys such as the Fancamp corridor (**Figure 2**) synvolcanic structure (Legault, 2003).

In the southern part of the study area (**Figure 1**), the sedimentary rocks of the Caopatina Formation (Roy Group) are interlayered with volcanic cycle 1 rocks (Mueller et al., 1989; Mueller & Donaldson, 1992). Volcanoclastic units observed in the same area however suggest that the Caopatina Formation may be in contact with unsubdivided units of volcanic cycle 2, and recent dating indicates that it may be a syn-Opémisca basin (David et al., 2006). Dedicated studies are necessary to determine the age and origin of the Caopatina Formation, and its contact relationships with volcanic cycles 1 and 2.

The base of volcanic cycle 2 consists of mafic lava flows, interbedded thin volcanoclastic lenses and pillow breccia of the Bruneau Formation (Leclerc et al., 2011; Picard & Piboule, 1986). It is overlain by the Blondeau Formation, which is a complex assemblage of intermediate to felsic volcanic, volcanoclastic and sedimentary units (Archer, 1983; Dembele, 1984; Duquette, 1964, 1982; Lefebvre, 1991; Tait, 1987). The Blondeau Formation is intruded by a series of three sills of the Cummings Complex (**Table 1**), which extend over 160 km in an E-W direction (Bédard et al., 2009; Dubé, 1990; Dubé & Guha, 1987; Duquette, 1982; McMillan, 1972; Pierre Pilote, 1986; Poitras, 1984; Watkins & Riverin, 1982). The top of volcanic cycle 2 comprises the Bordeleau Formation (Caty, 1979; Dimroth et al., 1985), a concordant sedimentary unit viewed as a transitional facies between the volcanic rocks of the Roy Group and overlying sedimentary rocks (Caty, 1978; Moisan, 1992).

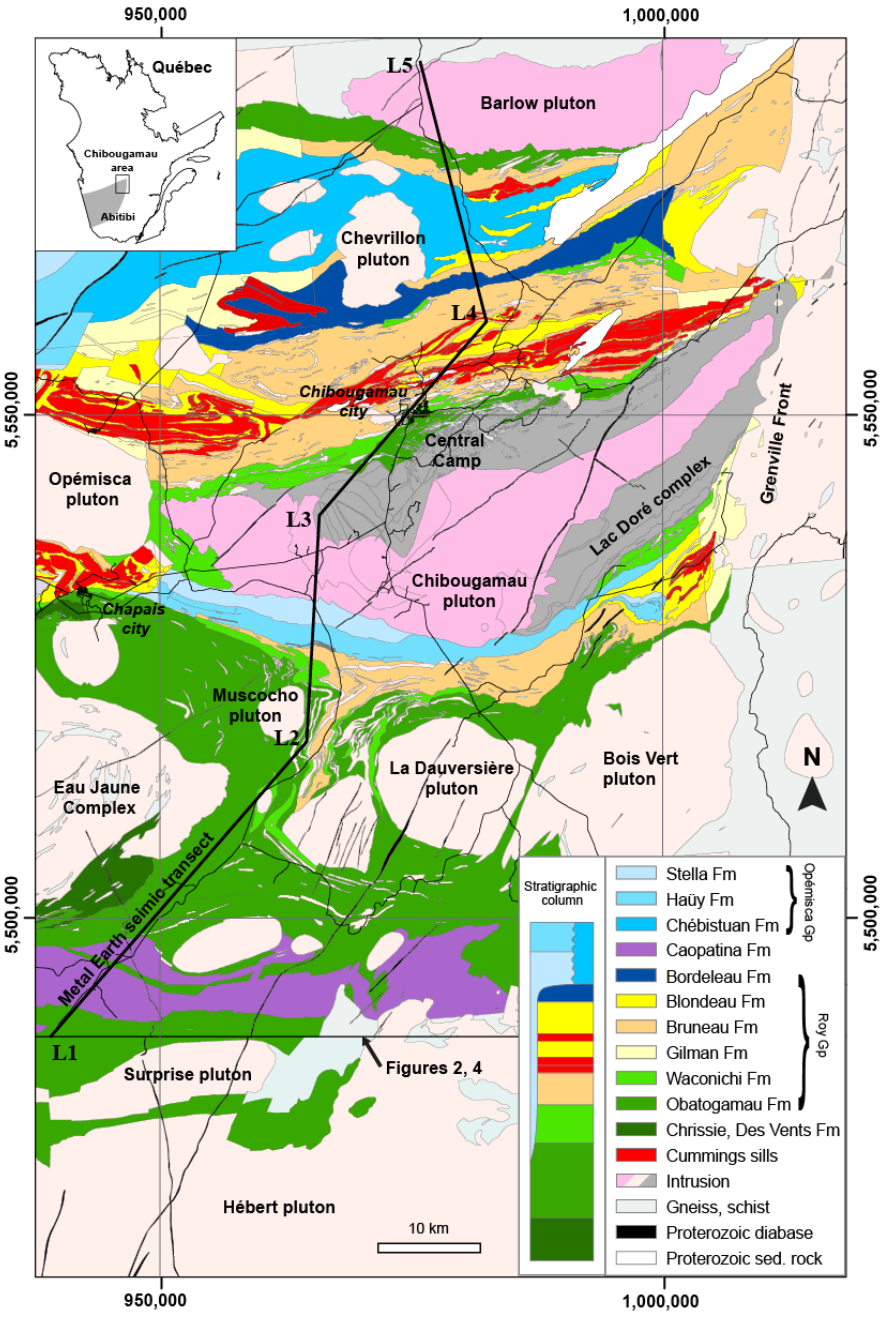

Figure 1. Geological map of the Chibougamau area, showing the main volcanic, sedimentary and intrusive phases. The geological map is modified from the Ministère de l'Énergie et des Ressources Naturelles (MERN), Québec (SIGEOM, 2020). The projection is UTM NAD83 Zone 18 N. The simplified stratigraphic column is inspired from the most recent stratigraphic interpretation (Leclerc et al., 2017). From base to top, the Cummings sills correspond to the Bourbeau, Venture and Roberge sills. The Caopatina Formation is not integrated to the stratigraphic column because it has a poorly constrained age and an unresolved relationship with the Opémisca Group. The Gilman Formation belongs to a former stratigraphic interpretation recently modified using new chemical and geochronological data (Leclerc et al., 2017).

Table 1. Stratigraphy of the Chibougamau area

Stratigraphy	Major rock types	Thickness	U/Pb age
Pre-Roy Group			
Chrissie Fm[1]	Mafic to felsic lava flows,	?	~2759 Ma [1][2]
Des Vents Fm	volcanoclastic deposits	2-2.5 km [2]	~2791 Ma [3]
Roy Group – cycle 1			
Obatogamau Fm	Mafic to intermediate lava flows	2-4 km [2, 4]	?
Waconichi Fm	Coherent to clastic, mafic to felsic, volcanic rocks	2.4 km [5]	~2730-2726 Ma [3, 6]
Roy Group – cycle 2			
Bruneau Fm	Mafic flows mostly	?	2724 Ma [7]
Blondeau Fm	Intermediate to felsic, volcanic to sedimentary deposits	2-3 km (north) to 0.5 km (south) [4, 8, 9]	<2721 Ma [10]
Bordeleau Fm	Volcanoclastic deposits, arenite, conglomerate		
Cummings sills	Three Ultramafic to mafic sills	<500 m, 250-1000 m, 450-750 m [9]	2717 Ma [3]
Roy Group (?)			
Caopatina Fm	Pelitic to siliciclastic sedimentary rocks	?	<2707 Ma [11] and older?
Opémisca Group			
Stella Fm	Sandstone, conglomerate		<2692 to
Haüy Fm	Sandstone, conglomerate, shoshonitic lava flows	<4 km	<2704 Ma [10, 12]
Chébistuan Fm	Sandstone, conglomerate		

[1] Fm stands for Formation

[2] References in the table: [1] (David et al., 2011); [2] (Mueller et al., 1989); ; [3] (Mortensen, 1993); [4] (R. Daigneault & Allard, 1990); [5] (Caty, 1975); [6] (Leclerc et al., 2011); [7] (D. Davis et al., 2014); [8] (Archer, 1983); [9] (Duquette, 1982); [10] (Leclerc et al., 2012); [11] (David et al., 2006); [12] (David et al., 2007).

Volcanic cycle 2 began with effusive volcanism (Bruneau Formation) followed by the development of a basin and small sub-aerial volcanic centers (Blondeau Formation) that shed volcanoclastic material into the basin (Archer, 1983). Alternatively, the Blondeau Formation and crosscutting Chibougamau pluton have been interpreted as a large central volcano underlain by a syn-volcanic pluton, with shallow to deep marine sediments deposited on the apron of the volcano (Dimroth et al., 1985; Mueller, 1991).

The Roy Group is topped by the Opémisca Group that accumulated in two sedimentary basins (Dimroth et al., 1985; Mueller, 1991; Mueller et al., 1989) (**Figure 1; Table 1**). Erosion of the volcanic islands progressively filled the basins with sediments. This formed the Bordeleau Formation (Roy Group) and then the Opémisca Group (**Figure 2**) as basin subsidence rate decreased (Dimroth et al., 1983) and the basin evolved from marine to sub-aerial (Dimroth et al., 1985; Mueller, 1991). The southern Opémisca basin contains clasts from the Chibougamau pluton, indicating that the pluton was eroded only 15 to 18 Ma after emplacement (R. Daigneault & Allard, 1990).

The Chibougamau area also contains intermediate to felsic intrusions. During the synvolcanic period, these intrusions are tonalite-trondjhemite-granodiorite (TTG) suites such as the Eau Jaune Complex (**Figure 1**) and tonalite-trondjhemite-diorite (TTD) suites such as the ca. 2714-2718 Ma Chibougamau pluton, which is characterized by multiple magma pulses and a poorly defined internal organization (Mathieu & Racicot, 2019). The ~2728 Ma Lac Doré Complex layered intrusion (Mortensen, 1993), which is a dominantly mafic complex with a coherent magmatic stratigraphy (Allard, 1976; Mathieu, 2019), also formed during the synvolcanic period.

Magmatism, in the syntectonic period, may postdate or may be coeval with the main sedimentary deposits (**Figure 3**). Only the shoshonitic lava flows observed in the Haüy Formation of the Opémisca Group (**Table 1**) are clearly syn-sedimentary units (Piché, 1985). Other plutons intrude the Roy and Opémisca groups (e.g., Muscocho and Chevrillon plutons; **Figure 1**). These include the 2696 Ma Barlow pluton (W. J. Davis et al., 1995), which consists of tonalite and monzodiorite cutting across the contact between the Abitibi and Opatica belts (Racicot et al., 1984). The Metal Earth project, using gravity inversion modelling, investigated the detailed geometry of these and additional intrusions, and showed that the main intermediate to felsic intrusions crossed by the seismic transect (the Chibougamau and Barlow plutons) continue downward to the mid-crust (Maleki Ghahfarokhi, 2019).

2.2 Magmatic evolution

The Chibougamau area is characterized by a synvolcanic period that lasted > 90 Myr, followed by a 20 Myr syntectonic period (**Figure 3**), as is typical in greenstone belts around the world (Laurent et al., 2014). Magmatic activity was likely episodic during both synvolcanic and syntectonic periods. Based on SiO_2 content, mafic and intermediate to felsic volcanic rocks dominate volcanic cycles 1 and 2, respectively (Leclerc et al., 2011, 2017).

Using the TAS (Le Bas et al., 1992), the AFM (Irvine & Baragar, 1971) and the Th/Yb vs Zr/Y (Ross & Bédard, 2009) diagrams, it was determined that the mafic lava flows (basalt to basalt-andesite) of the Roy Group and older units of the Chrissie and Des Vents formations have tholeiitic affinities (Leclerc et al., 2011, 2017). On REE and multi-element diagrams normalized to primitive mantle, they have flat patterns (Leclerc et al., 2017). In contrast, intermediate to felsic extrusive rocks of the Roy Group and older units have major element contents akin to those of calc-alkaline rocks and are enriched in the most incompatible elements, such as Th and La (Leclerc et al., 2017). Some of these rocks, however, display less fractionated trace element profiles and correspond to differentiated tholeiitic magma (Leclerc et al., 2017).

The only intrusive complex clearly coeval with volcanic cycle 1 (i.e., Lac Doré Complex) has a tholeiitic affinity (**Figure 3**). During volcanic cycle 2, tholeiitic intrusions also formed (e.g., Cummings sills) (Bédard et al., 2009), while several TTG and TTD suites intruded the volcanic pile. The onset of tonalite-dominated magmatism (TTG and TTD) is unconstrained in the Chibougamau area (**Figure 3**). The duration of syntectonic magmatism also needs better geochronological constraints, which is beyond the scope of this paper. As in other greenstone belts, synvolcanic magmatism is K-poor

(TTG suite), while the magmas of the syntectonic period contain more K (shoshonite flows, granodiorite, monzonite). Syntectonic magmatism is sub-alkaline in the Chibougamau area, with only the shoshonite flows of the Haüy Formation displaying an alkaline affinity.

2.3 Structural Geology

The Chibougamau area underwent four deformation events (R. Daigneault & Allard, 1990). Throughout the Abitibi greenstone belt, the first three events occurred at ~2.70 Ga during terrane assembly associated with the Kenoran orogeny (Dallmeyer et al., 1975). The D_1 deformation event is characterized by N-S to NNW-striking open synforms without associated axial planar cleavage (R Daigneault et al., 1990). These folds probably represent amplification or reactivation of synvolcanic structures such as the Fancamp corridor (**Figure 2**) (Legault, 2003).

The D_2 deformation event is coeval with peak greenschist facies metamorphism. Most regional folds in the Chibougamau area formed during the D_2 event, including the E-W-striking Waconichi, Chibougamau, Chapais and Druillettes synclines and the Waconichi, Chibougamau and La Dauversière anticlines (**Figure 2**). Several of those synclines mark deformed sedimentary basins, whereas the Chibougamau anticline was inflated, or domed, by magmatic injections (Chibougamau pluton) emplaced in the hinge of the anticline and further deformed during D_2 (R. Daigneault & Allard, 1990).

The folds have a subvertical and E-W-striking axial plane cleavage, which locally wraps around plutons that acted as resistant cores during the deformation. A near-vertical stretching lineation lies along the cleavage plane (R. Daigneault & Allard, 1990). Deformation is most intense around the plutons, along contacts between the Roy and Opémisca groups, in corridors spatially associated with gold showings (**Figure 4**), and within the contact zone between the Abitibi and Opatica subprovinces (R. Daigneault & Allard, 1990; Leclerc et al., 2017).

The formation of the regional folds and the intensification of their axial plane cleavage along lithological contacts was accompanied by the formation of E-W-striking reverse faults, although some of these faults may be older structures that were reactivated during D_2 (**Figure 2**). For example, the Barlow fault is interpreted as a basin-bounding syn-sedimentary fault that was reactivated as a reverse fault during D_2 (Dimroth et al., 1986). Other basin-bounding faults, such as the Kapunapotagan fault, are chloritised, sericitised and carbonatized (ankerite-rich) fault planes, similar to other hydrothermally altered gold-bearing D_2 faults across the Abitibi.

The D_3 deformation event, which correspond to the waning stage of the main deformation event (D_2), reactivated the east-west-striking faults as transcurrent strike-slip faults. The D_4 deformation event represents the ~1.1 Ga Grenville orogeny (Baker, 1980). It resulted in the formation of NNE-striking faults and amphibolite grade metamorphism near the Grenville Front (Kline, 1985) (**Figure 1**).

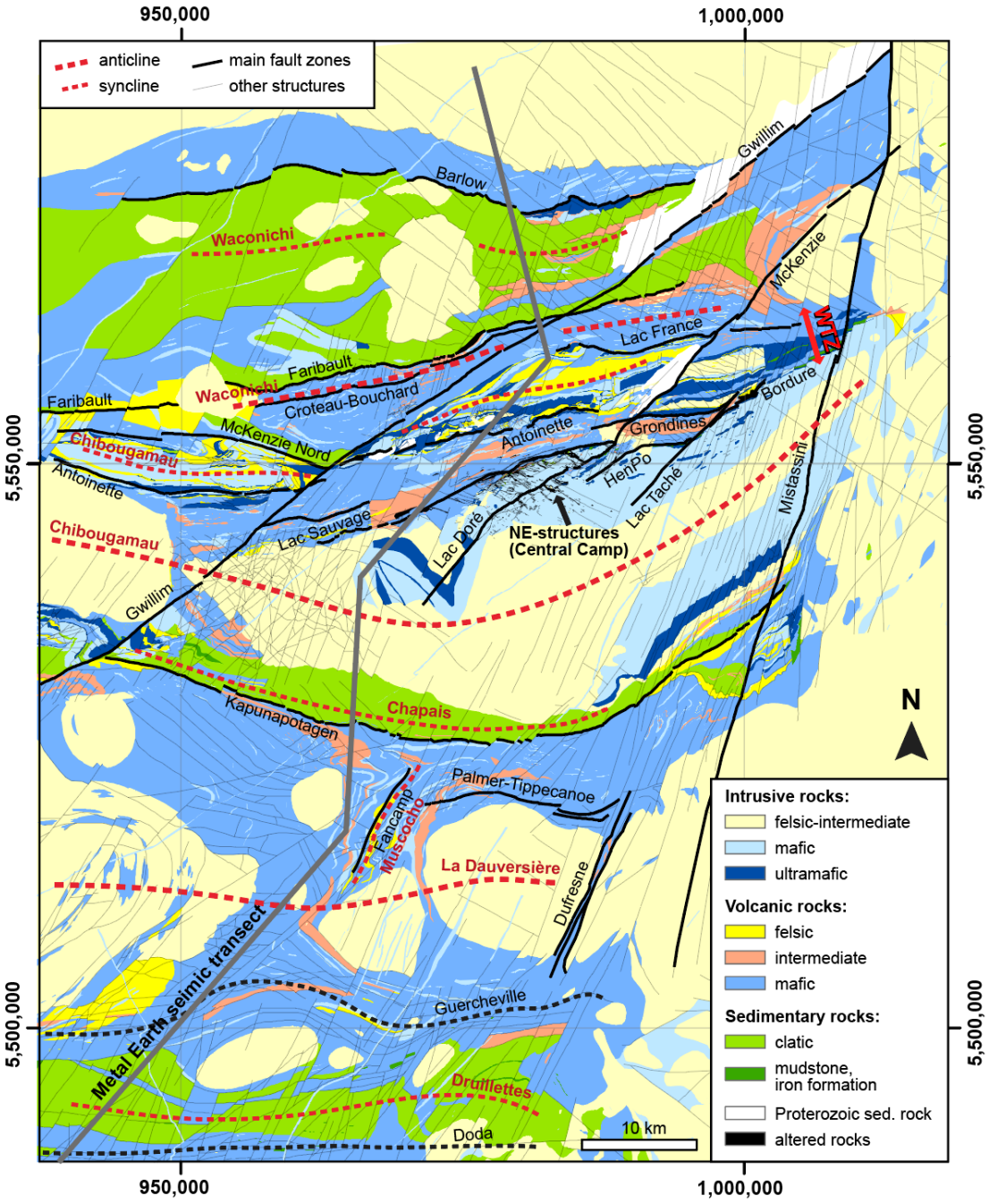

Figure 2. Lithologies and structures (SIGEOM, 2020), as well as main faults and deformation zones (R. Daigneault & Allard, 1990), of the Chibougamau area. The Barlow and Guercheville faults (Mueller et al., 1989), as well as the Doda fault zone (Hamid, 1993), are approximately located using published maps (Réal Daigneault, 1996). Most of the E-W-structures are thick deformation corridors and are drawn as thin lines for clarity. The red dashed lines correspond to the axial traces to the main folds. The following abbreviations are used: 'Bordure' refers to a fault located along the northern border of the Lac Doré Complex, WTZ refers to the Waconichi tectonic zone and 'HenPo' is the Henderson-Portage fault.

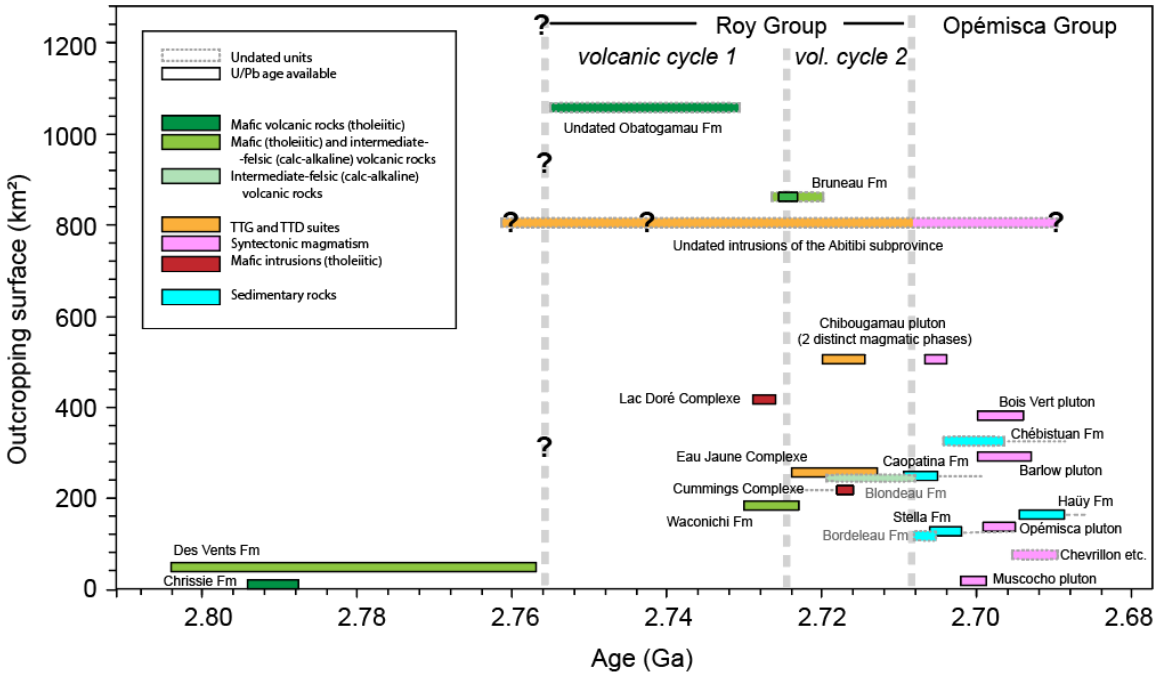

Figure 3. Binary diagram showing the surface area occupied by the main lithologies on **Figure 1** against the radiogenic ages available in the MERN dataset (SIGEOM, 2020). A total of 30 U/Pb ages (9 of which in the Waconichi Formation) were compiled from the MERN database (SIGEOM, 2020) and an approximate age is attributed to the undated units. Magmatic affinities were compiled for the volcanic rocks (Leclerc et al., 2017; Potvin, 1991) and, for intrusive rocks, was attributed as follows: 1) large-volume synvolcanic intrusive complexes dominated by tonalite and/or diorite are given the general designation TTG and/or TTD suites; and 2) other plutons with variable volumes (e.g., monzodiorite, granodiorite) are designated 'syntectonic intrusions'. The following abbreviations are used: 'Fm' stands for Formation; 'Chevrillon etc.' refers to the Chevrillon pluton and to the other intrusions emplaced in the Chébistuan Formation. Note that undated plutonism and volcanism (e.g., Obatogamau Formation) may not be as continuous as is suggested by the diagram.

3 Methodology and results

3.1 Acquisition of seismic reflection data

The Metal Earth seismic program used existing roads with 2-D surveys designed to provide improved lateral and vertical seismic wave resolution of both near-surface and deeper crustal structures (Cheraghi et al., 2019). Where coincident with older Lithoprobe seismic profiles, resolution within the upper- to mid- crust along the Metal Earth seismic profiles equals or surpasses the older data (Naghizadeh et al., 2019). Metal Earth seismic and magnetotelluric joint surveys were acquired as regional (R1) and high-resolution (R2) surveys. The geometrical attributes of both survey types, as well as the processing performed to produce the migrated sections (**Figure 5**), are specified in detail elsewhere (Cheraghi et al., 2018; Naghizadeh et al., 2019).

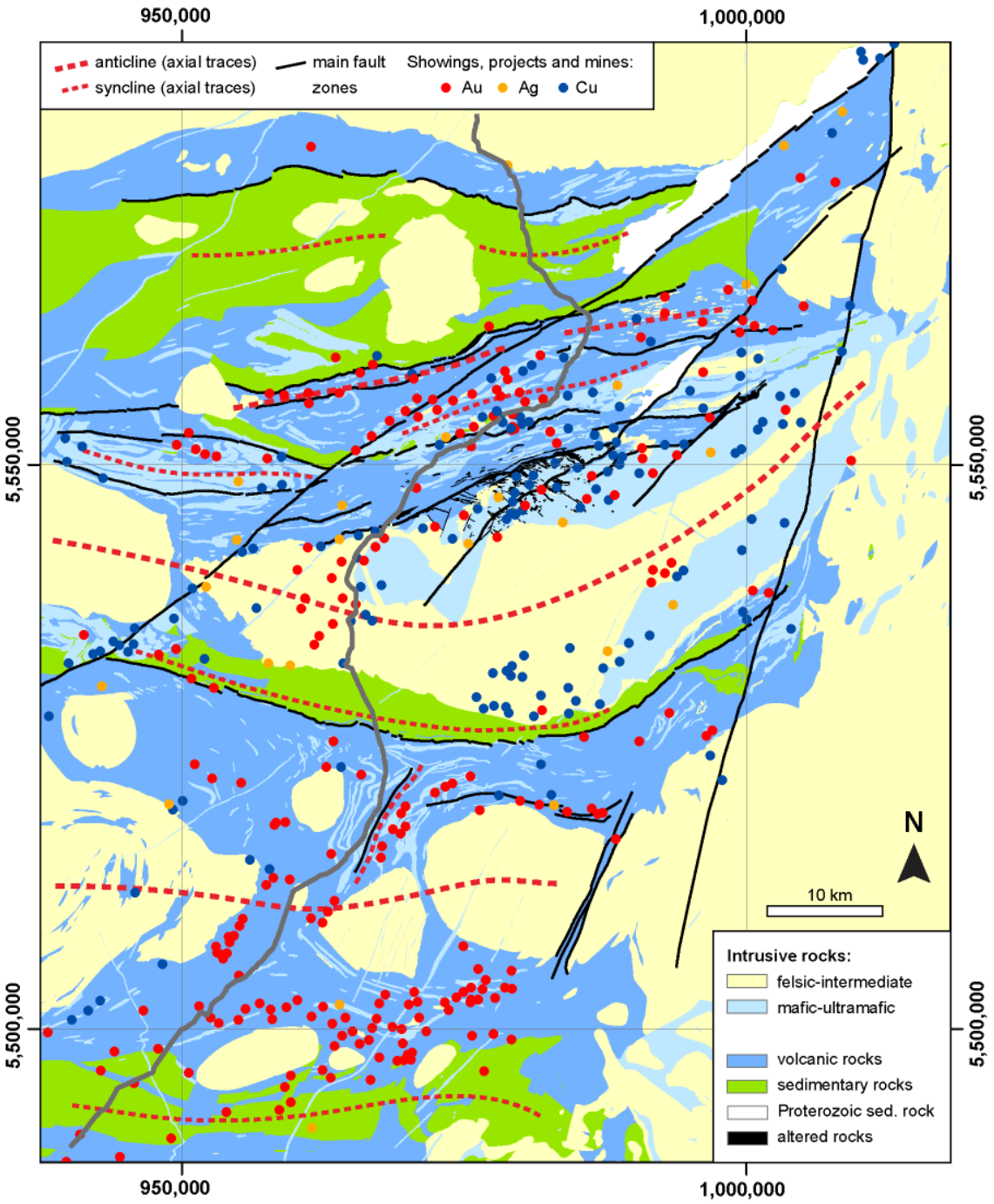

Figure 4. Main lithologies, structures and Au-Cu-Ag-showings of the Chibougamau area (SIGEOM, 2020). A part of the Au showings aligns parallel to the main E-W faults and deformation zones, such as the Guercheville, Plamer-Tippecano, and Antoinette – Croteau – Lac France faults zones. Other Au showings, as well as most Cu showings and mines, are spatially associated with the Chibougamau pluton (porphyry-style of mineralization) (P. Pilote, 1995; P. Pilote et al., 1998) and the Cummings sills (Opemiska-style of mineralization) (Leclerc et al., 2012).

The R1 Chibougamau survey presented here is not located near any previous Lithoprobe or Discovery Abitibi profiles and thus provides new insights into deep crustal structures. The interpreted profile is 113 km long, starting within the Barlow pluton in the north (Abitibi to Opatica subprovinces contact) and ending in the Caopatina basin in the south. Data were acquired along 162 km of foresting roads and projected onto four straight segments (113 km total length) during common-depth-point (CDP) processing (**Figure 1**). This profile provides a complete section across the eastern extremity of the E-W-striking Matagami-Chibougamau greenstone belt.

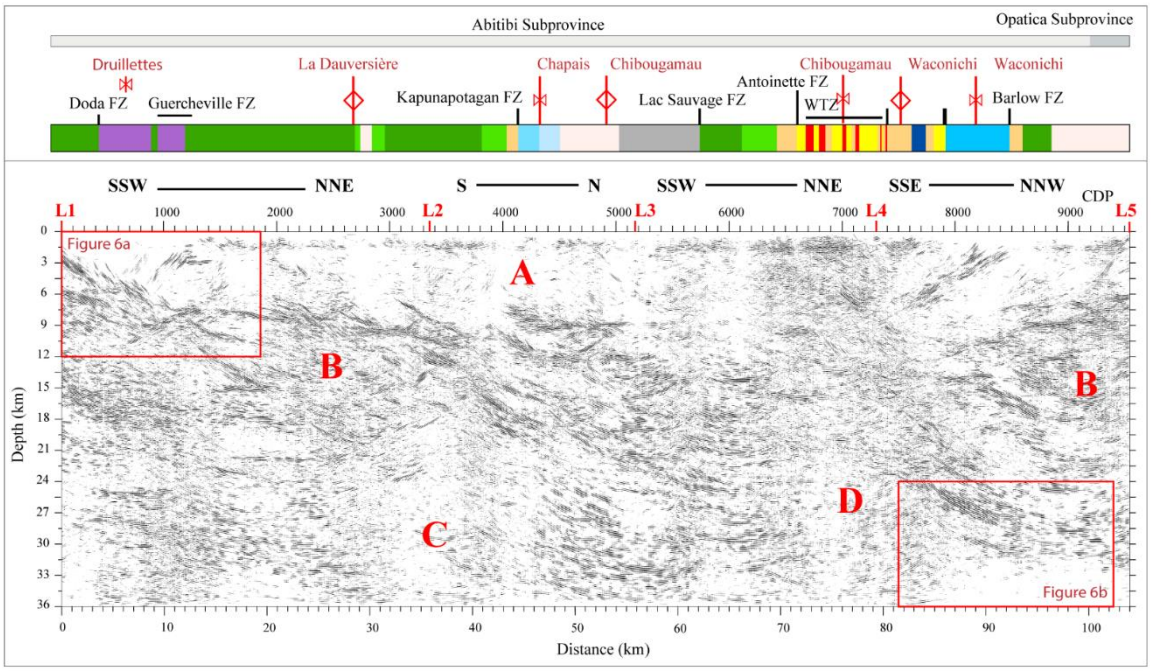

Figure 5. The migrated Metal Earth R1 seismic profile of the Chibougamau area (for full resolution, see supporting information files S1, S2 and S3). Time-varying and intense coherency filters have been applied (see text for details). Markers L1 to L5 are located on **Figure 1** and zones A to D are described in the text. The stratigraphic units, lithologies and structures intersected by the Metal Earth seismic profile (b) were extracted from the MERN dataset (SIGEOM, 2020) using the ArcGIS software, and served as a basis to interpret the seismic profile (legend as shown on **Figure 1)**.

We applied a pre- and post-stack processing steps similar to previously introduced processing (Schmelzbach et al., 2007) to remove coherent/incoherent noise and migrate the data (**Table 2**). First arrivals within the range of 0-15 km were picked automatically and edited manually. A median filter was designed to remove shear waves and ground-roll. Surface-consistent deconvolution was applied to remove the effect of the seismic source. Refraction and residual static corrections applied prior to DMO (dip moveout) corrections further enhanced the coherency of the reflections, especially in the shallower part of the section. DMO corrections used a velocity of 5,500 $m.s^{-1}$ chosen based on several tests between 5,000-6,000 $m.s^{-1}$ with an increment rate of 100 $m.s^{-1}$. Velocity analysis after DMO corrections used a constant velocity stacking algorithm to pick velocities that generate the most coherent reflections in both shallow and deeper parts.

After the migration process, we applied a time-varying frequency filter to enhance signal-to-noise (S/N) ratio of the imaged reflections (**Table 2**); the criteria to choose the filter is based on our evaluation of the frequency band in different time/depth of the migrated section to find a band with the highest energy in a dominant frequency band.

Frequency spectra calculated within nine windows have bandwidths ranging from 17-75 Hz in the uppermost crust to 10-30 Hz in the lowermost crust (**supporting information S1**). When examining details of the R1 section, a bandpass filter of 10-20-55-75 was applied for times 0-4s (0-12 km), while for times 4-8 s (12-24 km) and 8-12 s (24-36 km), lowpass filters were applied to preserve signal at a range of 5-40 Hz and 5-30 Hz, respectively. The four stacked seismic section segments of the R1 Chibougamau survey were each migrated (phase-shift) at a constant velocity of 5,500 $m.s^{-1}$. Depth conversion used a constant velocity of 6,000 $m.s^{-1}$. Moderate (**supporting information S2**) and intense (**Figures 5, 6**; **supporting information S3**) coherency filters (Milkereit & Spencer, 1989) provided alternative versions of the R1 section.

As noted out above, the Metal Earth program was designed to improve resolution in the upper crust. Processing was designed accordingly and the results should not be used to reliably define the Moho in the study area. The location of the Moho can, however, be inferred using the data from a nearby permanent broadband station (CHGQ) that was used for receiver function analysis of the Moho. The automated Earthscope Automated Receiver Survey (Trabant et al., 2012) calculates 35 ±1.2 km Moho depth. Multi-azimuthal receiver function analysis at CHGQ indicates a range of 33-38, with an average of 35.6 ±1.6 km (D. Snyder, unpublished data), thus providing consistency (**Figure 6b**).

3.2 Reflectors, geological units and faults

Seismic waves are sensitive to physical properties of rocks, particularly seismic wave propagation and density. For the Chibougamau area, characteristic seismic wavelengths of 110-380 m derive from measured frequency spectra (17-55 Hz) and from velocities that optimized stacking (6,000-6500 $m.s^{-1}$). The seismic wavelength determines the resolution and thus the scale at which reflectors between contrasting rock types can be observed (Eaton et al., 2010). Typical vertical resolution is one-quarter of the seismic wavelength, and thus 30-110 m, increasing with depth within the Chibougamau seismic section. Lateral resolution on migrated sections is a half wavelength (Yilmaz, 2001), so also varies with depth and, in the study area, is 60-200 m. Reflections can also come from the sides of the survey line and this so-called Fresnel zone is several kilometers in diameter within the mid and lower crust.

In the Chibougamau area, prominent reflectors were identified visually on the seismic profile and correlated with surface geological units and mapped faults (see next sections). Most structures and lithological units strike E-W at surface, so the seismic transect was designed to follow roughly N-S roads (**Figure 2**). A notable exception is the Fancamp corridor area (L2 marker), where the lithological contacts are oriented NNE-SSW and are sub-parallel to the seismic profile (**Figure 2**). The Fancamp corridor, however, has a limited lateral (E-W) width of 5-10 km (**Figure 1**) and may not continue significantly at depth.

Another exception is the Chibougamau syncline area, located immediately south of the L4 marker (area D on **Figure 5**), where the road and transect are sub-parallel to lithological contacts, cross through a paper mill, and glacial till of increased thickness is observed. These surface features may all be partly responsible for the decrease in reflectivity in area D (**Figure 5**). In addition, the main near-surface lithologies are the Blondeau Formation, dominated by graphite-rich and felsic rocks, and ultramafic to mafic sills of the Cummings Complex (**Figure 1**). Abundant lithological contacts between units of strong impedance contrast may have refracted seismic waves and further attenuated the signal at greater depth, partly explaining the paucity of reflectors in area D (**Figure 5**). Other geological processes as discussed below may have degraded the impedance contrast between lithologies in this low-amplitude zone.

Table 2. Processing parameters and attributes for the Chibougamau regional (R1) survey

	Chibougamau R1 survey
1	Reading data in SEGD format (correlated) and converting them to SEGY format
2	Setup geometry
3	Trace editing (manual)
4	First arrival picking and top muting (0-15000 m)
5	Elevation and refraction static corrections (replacement velocity 5200 m/s, V0 1000 m/s)
6	Spherical divergence compensation (velocity power of 2 and travel time power of 1, V^2t)
7	Median velocity filter (1400, 2600, 3000 m/s)
8	Band pass filter (5-20-60-85 Hz)
9	Airwave filter
10	Spectral whitening (10-20-60-70 Hz)
11	Surface-consistent deconvolution (filter length: 100 ms, gap: 19 ms)
12	Trace balancing
13	AGC (window of 150 ms)
14	Velocity analysis (iterative)
15	Surface consistent residual static corrections
16	DMO corrections (constant velocity of 5500 m/s)
17	Velocity analysis (iterative, 5000-6500 m/s)
18	Stacking
19	Coherency filter (F-X deconvolution, filter length of 19 traces)
20	Trace balancing
21	Phase shift time migration (constant velocity of 5500 m/s)
22	Time-Varying filter [1]
23	Coherency/Skeletonization [2] (lateral sliding window: 49 traces, dip limit: 2.2 ms/m)
24	Time to depth conversion (constant velocity of 6000 m/s)

[1] Band pass filter (10-20-55-75 Hz, 0-4 s), low pass filter (40 Hz, 4-8 s) and low pass filter (30 Hz, 8-12 s)

[2] (Milkereit et al., 1989)

3.3 Interpretation of the main reflectors

The general structure of the seismic section (**Figure 5**) consists of: 1) an upper-crust extending to 6 to 13 km depth (A), characterized by sub-horizontal reflectors of

limited N-S extent, with some notable exceptions described below; 2) a mid-crust that extends down to 16 to 30 km depth (B) where the most prominent reflectors are concentrated; 3) a lower-crust (C) that contains few prominent reflectors; and 4) a localized area of lesser reflectivity (D) where seismic waves are apparently attenuated (see previous section). The mid-crust layer has an apparent shallow dip (7°) directed toward the north, except in the northernmost part of the profile, where it dips toward the south at 16° (**Figure 5**). In this section, all dip values correspond to apparent dips.

Interpretation of the Metal Earth seismic profile will emphasize the areas with most abundant reflectors, as well as the low reflectivity areas, which together we number 1 to 6 (**Figure 7a**). Areas 1 and 2 are located in the northern part of the profile and comprise deep (>12 km depth) reflectors that dip shallowly (27° to 22°) toward the north. South-dipping reflectors are also observed, including the shallow dipping (16°) mid- to upper-crustal contact and 34° dipping near-surface reflectors (area 2) that correlate to the Barlow fault at surface (Bedeaux et al., 2020). These north- and south-dipping reflectors form a wedge geometry within the northern part of the profile.

The mid-crust (area 3) is dominated by north-dipping reflectors. The most prominent and continuous reflectors are observed along the mid- and upper-crust contact, whereas the mid- to lower-crust contact (area 3a) appears much less reflective (**Figure 7a**). In the mid-crust section, most reflectors dip 7° or 20° toward the north and are imbricated. Additional reflectors dip 18° toward the south (area 3b) and offset north-dipping reflectors with a normal fault motion (**Figure 6a**).

In area 4 in the upper crust, strong reflections are spatially associated with the mapped Guercheville and Doda fault systems (**Figure 7a**). The north-dipping (37°) and south-dipping (50°) reflectors may correspond to conjugate faults. Further north, several zones of low reflectivity occur in the upper crust. Below the prominent reflection set associated with the Barlow fault (area 2), apparent low reflectivity could be a processing (gain shadow) artefact. Elsewhere (areas 5a to 5d), low reflectivity correlates with sedimentary rocks (areas 5a and 5c) and with the Chibougamau pluton (area 5d) at surface. Area 5b is correlated with a small intrusive plug at surface and may correspond to a larger buried intrusion (**Figure 7b**).

The main zone of decreased reflectivity is area 6a (**Figure 7a**) that extends from the upper to lower crust regions, with particularly attenuated signal below 15 km. Some reflectors extend faintly through this zone indicating, despite possible signal attenuation attributable to surficial features and sub-surface lithologies (see section 3.2), crustal-scale geological features such as alteration zones or magmatic systems similar to these interpreted elsewhere (Heinson et al., 2018; Snyder et al., 2008). Signal is also attenuated below 18 km depth in area 6b (**Figure 7a**). This area underlies the pluton alignment observed in the core of the La Dauversière anticline (**Figure 2**). Area 6a may correspond to the most active magmatic system of the study area and area 6b, which is restricted to the lower crust region, may correspond to a magmatic system that is less voluminous (or that remained active for a lesser amount of time) than the magmatic system of area 6a.

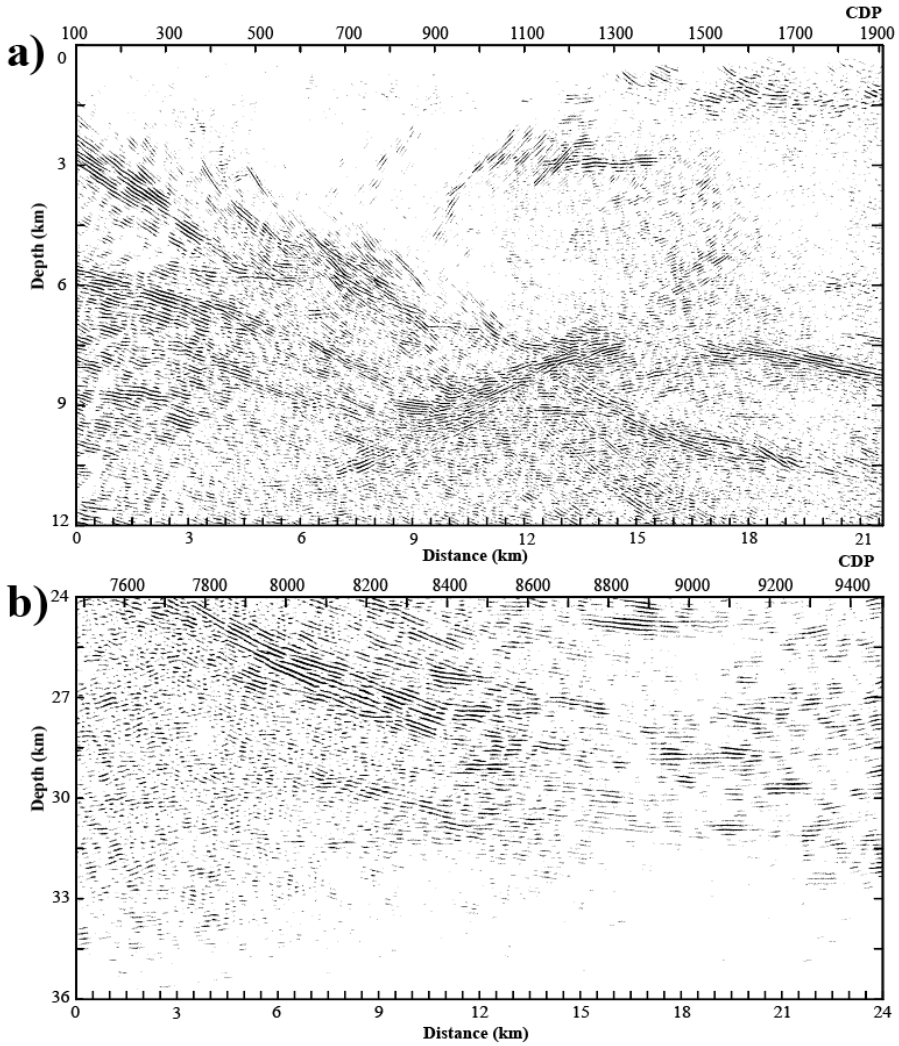

Figure 6. (a) Detail of the upper crust in the southern part of the transect showing numerous distinct, intersecting reflectors at 6-10 km depths. Sense of offset indicate normal motion along a fault cutting low-angle reflectors interpreted as reverse faults. Data were processed as in previous figure, but with a 20-55 Hz bandpass filter. (b) Detail of the lowermost crust at the northern end of the transect showing relatively sharp decrease in reflectivity with depth at 32 km, within rocks interpreted as lower crust gneisses with little internal impedance contrast. The seismic section was depth converted assuming 6,000 $m.s^{-1}$ velocity (depth may be underestimated here). Data processed as in previous figure, but with a 30 Hz lowpass filter. For full resolution and additional detail views, see supporting information file S1.

3.4 Interpretation of lithological contacts

Interpretation of the Metal Earth seismic profile related the main reflectors to known lithological contacts, faults and folds at surface (**Figure 7b**). The supracrustal rocks appear drawn as a folded volcano-sedimentary succession with limited northward and southward extent, which thickens (14 km thick) in the Chibougamau and Waconichi

synclines area. Within this supracrustal sequence, the main faults exposed at surface that can be related to prominent reflectors are the Barlow and Guercheville fault systems. The most prominent upper crustal reflectors connect with the Barlow fault, which has been recently documented as a reverse fault that accommodated ductile N-S shortening prior to exhumation of the northern part of the study area toward the end of the cratonisation process (Bedeaux et al., 2020). The Guercheville fault is subvertical and accommodated vertical motion (Réal Daigneault, 1996).

The E-W Doda fault (**Figure 2**) dips steeply toward the north at surface and accommodated shortening, followed by dextral strike-slip motion (Hamid, 1993). Shallow (37°) north-dipping reflectors beneath this fault may correspond to another, undocumented fault system located south of the Doda fault. These three fault systems are proximal to sedimentary rocks (Caopatina Formation and Opémisca Group) and may represent basin-bounding faults reactivated by the main shortening event (Dimroth et al., 1986). The Kapunapotagan fault is another prominent structure at surface. This fault is sub-vertical, which may explain the lack of associated reflections.

Interpretation of lithological contacts (**Figure 7b**) used the MERN geological map (**Figure 1**) and locations of known facing directions and folds (**Figure 2**). In the upper crust, sedimentary basins (Opémisca Group and Caopatina Formation) are interpreted as synforms with unknown downward extents. The rocks of volcanic cycle 2 are mostly exposed in the northern part of the study area, in the core of the Chibougamau and Waconichi synclines, and are underlain by volcanic cycle 1 (**Figure 7b**). The upper-crust comprises mostly lava flows of the Obatogamau Formation (cycle 1) and, possibly, undifferentiated older volcanic rocks (**Figure 7c**) such as those exposed in the La Dauversière syncline (**Figure 1**).

As described above, the most disrupted zone occurs in the upper part of the mid-crust, where multiple imbricated reflectors are observed (**Figure 7a**). These reflectors are interpreted as structures superimposed on a major lithological contact, i.e., contact between volcano-sedimentary supracrustal rocks and mid-crustal rocks. The mid-crust region is characterized by a large number of shallowly north-dipping reflectors (**Figure 7b**). It underlies both the Opatica and Abitibi subprovinces. Ever increasing thickness to the north suggests imbrication between the Opatica and Abitibi crusts (area 2; **Figure 7a**). The mid-crust has the overall geometry of a large-scale syncline, with 7°N and 16°S dipping (apparent dips) southern and northern flanks, respectively. The overlying supracrustal rocks are here interpreted as folded at a smaller scale compared to the mid-crustal layer, with three anticlines and four synclines mapped at surface (**Figure 2, 7b**).

The location of the main magmatic systems can also be interpreted using surface lithologies. The main intrusions are the Chibougamau pluton and the Lac Doré Complex next to marker L3, the Barlow pluton to the north, and a buried intrusion to the south (area 5b; **Figure 7**). At depth, weak reflectivity may relate to magmatic systems that fed these plutons (areas 6a and 6b). These magmatic systems (area 5a mostly) cut through the main reflectors and through the large-scale (~100 km amplitude) syncline (mid crust region), possibly because N-S shortening (i.e., main deformation event, D_2) preceded or was coeval with magmatic activity.

4 Discussion

In this section, the structure and lithology of the Chibougamau area, which forms the eastern part of the E-W Matagami-Chibougamau greenstone belt, are interpreted with comparison to the crust imaged in the Matagami area using improved resolution of crustal architecture provided by the Metal Earth seismic section. Geodynamic processes relevant to both areas are then discussed.

4.1 Supracrustal sequence and upper crust region

Interpretation of seismic reflection data indicates that the Abitibi upper crust extends to 6 to 13 km depth in the Chibougamau area, consistent with depth extents based on gravity modelling, and likely consists of supracrustal rocks. The thickest upper crust occurs north of Chibougamau city, where volcanic cycle 2 is best exposed (marker L4; **Figure 7**). The thinnest upper crust lies north and south of the study area, where it is bounded by gneisses of the Opatica subprovince (plutonic belt) to the north and by the Hébert pluton to the south.

The upper crust contains several reflectors and areas of low-amplitude reflectivity that help to interpret its structure and lithology. The main faults associated with strong reflectors are the Barlow and Guercheville faults, both of which dip shallowly toward the south. Shallowly dipping faults are uncommon throughout the Abitibi greenstone belt, but have been documented in the northwestern part of this belt in the Matagami area, where they are interpreted as low-angle thrusts (Lacroix & Sawyer, 1995). Given the overall scarcity of thrusts in Abitibi, these thrusts suggest a common structural evolution for the Matagami-Chibougamau greenstone belt.

The Doda fault, the Kapunapotagan fault and the Waconichi tectonic zone (**Figure 2**), are all mapped as subvertical and, as a consequence, are not directly associated with reflectors. Most of the faults mentioned here may correspond to early basin-bounding normal faults reactivated during the main shortening event D_2 (Mueller et al., 1989). These faults also record late (D_3) dextral (e.g., Doda fault) and normal (e.g., Barlow fault) motions (Bedeaux et al., 2020; Hamid, 1993).

The main lithologies exposed at surface are volcanic rocks. The rocks of volcanic cycle 2 exposed in the Chibougamau syncline (marker L4; **Figure 7b**) do not associate with strong reflectors. This result is surprising because the Blondeau Formation (felsic) intruded by the Cummings sills (gabbro) results in contacts between mafic and felsic rocks expected to produce strong reflections. For example, the Lithoprobe program recorded strong reflectivity at laterally continuous lithological contacts characterized by large impedance contrasts; e.g., gabbro-rhyolite contacts (Adam et al., 1998; Eaton et al., 2010) and mafic sills intruding intermediate composition rocks in the mid-crust (Calvert & Ludden, 1999). In the Chibougamau area several faults (Waconichi tectonic zone) intersect the mafic and felsic rocks of volcanic cycle 2, possibly explaining their inconspicuous reflectivity and indicating that the poorly documented Waconichi tectonic zone may have accommodated a significant amount of displacement.

Similar to volcanic cycle 2, the rocks of volcanic cycle 1 do not associate with strong reflectivity, except for some shallow sub-horizontal reflectors (**Figure 7a**). This part of the crust contains zones of weak reflectivity associated with sedimentary rocks

(areas 5a and 5c; **Figure 7a**). This lack of reflectivity may be explained by the mapped sub-vertical attitude of the sedimentary units and by the lack of large impedance contrasts between units dominated by conglomerates and sandstones.

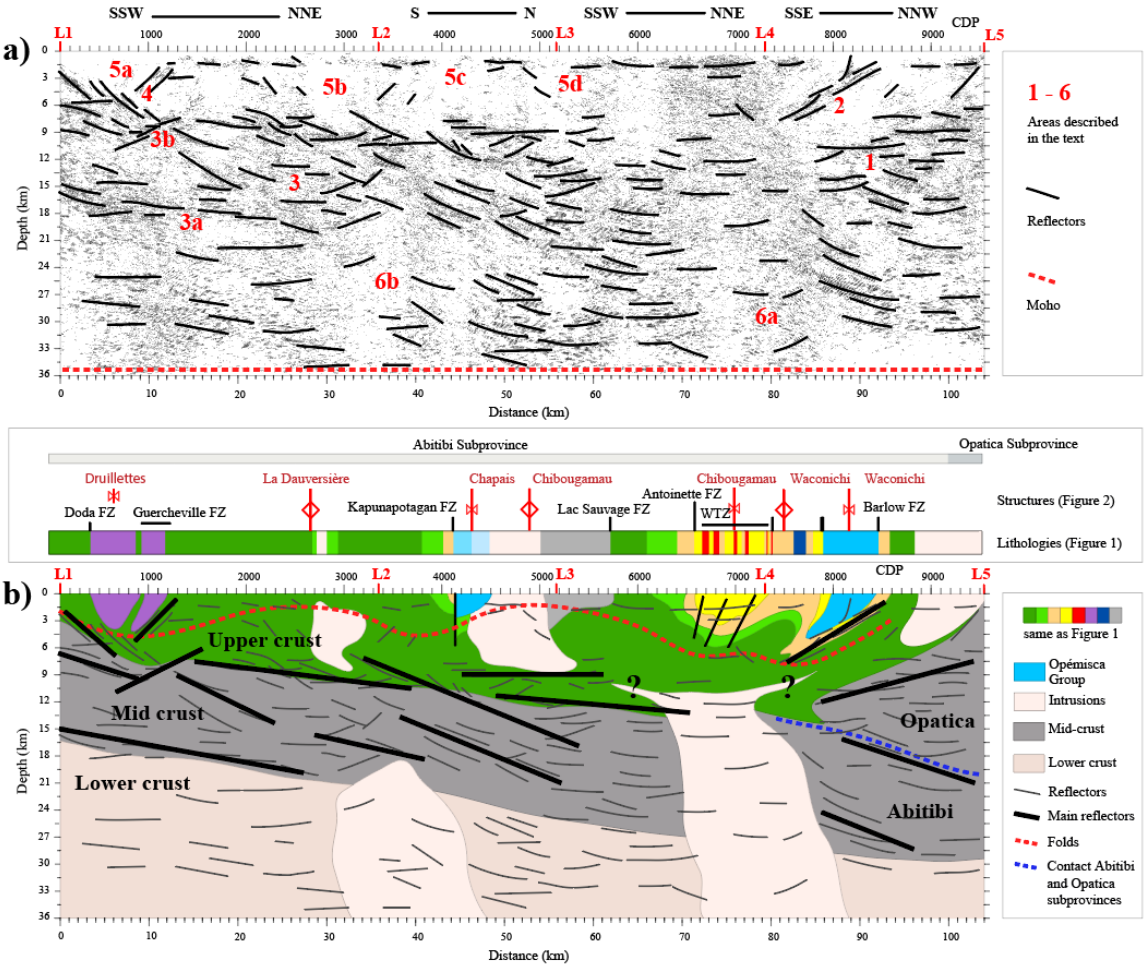

Figure 7. Interpreted seismic profile showing the main reflectors (a) and possible extensions of surface geology at depth (b). The stratigraphic units, lithologies and structures intersected by the Metal Earth seismic profile (b) were extracted from the MERN dataset (SIGEOM, 2020) using the ArcGIS software, and served as a basis to interpret the seismic profile. The Moho (a) is located at 35 km using receiver function analysis (Trabant et al., 2012). The WTZ abbreviations refers to the Waconichi tectonic zone.

Other areas of weak reflectivity could map packages of rocks with poor internal organization, i.e., magma intrusions such as the Chibougamau pluton (area 5d; **Figure 7**). A buried intrusion (area 5b) is also suggested and may belong to the alignment of intrusive complexes exposed in the core of the La Dauversière anticline (**Figure 2**). This interpretation uses constraints from modeling of subsurface rock units performed using gravity, magnetic and conductivity data (Maleki Ghahfarokhi, 2019). In particular,

gravity models constrained the northward extent of the lower part of the Chibougamau pluton in area 5d (**Figure 7**).

The seismically interpreted geometry of the Barlow pluton (**Figure 7b**) also coincides with the interpretation derived from gravity models (Maleki Ghahfarokhi, 2019). It is proposed that magma infiltrated south-dipping faults located in the upper crust or at the upper- to mid-crust contact as it ascended toward the surface during the syntectonic period to form the Barlow pluton. This interpretation implies that south-dipping faults and other structures formed prior to 2696 Ma (crystallization age of the Barlow pluton) (W. J. Davis et al., 1995). The south-dipping faults were either (1) reverse faults at the time, as magma intrusions are known to infiltrate active reverse faults (Galland et al., 2003), or (2) normal faults that accommodated the exhumation of the Opatica plutonic belt to the north.

The mapped large-scale open folds of the Chibougamau area also characterize the interpreted section (see red dashed line; **Figure 7b**). As interpreted previously (R. Daigneault & Allard, 1990), we argue that the La Dauversière and Chibougamau anticlines (and intercalated synclines) initiated as magma-cored doming during the synvolcanic period, mostly during volcanic cycle 2 (~2.73 – 2.71 Ga) according to the age of the main plutons (**Figure 3**). These folds then tightened and amplified during the main N-S shortening event (D_2). This interpretation points toward deformation that initiated during the synvolcanic period and to shortening that initiated during the syntectonic period or earlier.

4.2 Structure of the crust

4.2.1 General structure of the crust

The Chibougamau profile has features similar to those of the Abitibi Lithoprobe profiles. Most Lithoprobe profiles are characterized by three distinct layers of crust (Lacroix & Sawyer, 1995; Ludden et al., 1993; Percival et al., 1989). These correspond to an upper crust (< 6-9 km depth) characterized by listric thrusts and imbricated rock packages, a mid-crust (3-12 to 12-25 km depth) dominated by low-angle thrusts, ramps and culmination folds, and a less-reflective lower-crust (>12-25 km) with a similar structure (Lacroix & Sawyer, 1995). In the Chibougamau area, the upper (< 6-13 km depth), mid (up to 16-30 km depth) and lower (up to ~35 km depth) crusts have similar vertical extents.

That steeply-dipping faults at surface link to flatter structures at depth on most Lithoprobe profiles (Ludden & Hynes, 2000) does not apply to the Chibougamau area, where both the upper- and mid-crust are characterized by shallow-dipping reflectors and folded supracrustal rocks (**Figure 7b**). Imbrication is postulated for the northern part of the study area only, where the structure of the mid-crust region (areas 1 and 2; **Figure 7a**) suggests wedging of the Opatica into the Abitibi crust.

Most crustal sections around the world have a complex fine-scale layering (lenticular granitoid bodies, deeply buried sedimentary sequences, etc.) that can cause deep reflections (Fountain & Salisbury, 1981) and that represent the imbrication of terranes with contrasting compositions (Khazanehdari et al., 2000; Rutter et al., 1999).

The Lithoprobe seismic sections also comprise an Abitibi mid-crust region composed of metasedimentary and igneous rocks imbricated during subduction-driven horizontal tectonics (Bellefleur et al., 1995; Calvert & Ludden, 1999; Ludden et al., 1993). Compared to these examples, the Chibougamau profile has a very different, more homogenous, architecture, with no evidence of deeply imbricated sedimentary packages.

The gently northward-dipping reflectors observed in the mid-crust of the Chibougamau Metal Earth profile are similar to those observed on Abitibi Lithoprobe line 28/29/48, located 250 km to the west in the Matagami area (Bellefleur et al., 1995; Calvert & Ludden, 1999; Lacroix & Sawyer, 1995). These reflectors are thought to form by underthrusting and accretion of the Abitibi crust beneath the Opatica crust at depth, while the supracrustal rocks of the Abitibi belt overly the Opatica plutonic belt (Calvert & Ludden, 1999; Sénéchal et al., 1996). A similar interpretation can now be proposed for the Chibougamau area, which also displays a wedge geometry in its northern part, with the Opatica mid-crust acting as an indenter (**Figure 7b**). The northern part of the Abitibi greenstone belt (the Matagami-Chibougamau greenstone belt) thus probably has consistent structure over its whole length (430 km).

As noted out above, the Metal Earth program was not designed to image the Moho, which is located at ~35 km depth in the study area (Trabant et al., 2012). This correlates with signal attenuation on the Metal Earth seismic section (**Figure 6b**). In general, the Moho in Archean crust is located at 38-40 km depth and, at the scale of the Abitibi greenstone belt, the crust has a thickness of 35-40 km according to the synthesized results of the Lithoprobe program (Ludden et al., 1993). The crust is thinner adjacent to the Grenville Front as a consequence of post-Grenville orogeny extension (Martignole & Calvert, 1996), explaining the ~35 km Moho depth in the study area.

4.2.2 Detailed structure of the crust

Many reflectors with shallow apparent dips characterize the Chibougamau R1 Metal Earth profile. The profile was designed to cut across the main faults, fold axes and lithological contacts at a high angle, so these apparent dips probably approach true dips. Most of these reflectors likely formed during the main N-S Neoarchean shortening event (D_2). Because the Chibougamau area neighbors the Grenville Front, some of the faults associated with the main reflectors may also relate to the Proterozoic Grenville orogeny (D_4), about 1.5 Ga after craton stabilization. Faults associated with the D_4 event are sub-vertical NNE-SSW striking structures at surface (**Figure 2**) and have undocumented attitudes at depth.

However, the general attitude and distribution of the reflectors observed on the Chibougamau profile resemble reflectors observed in the Matagami area, 250 km to the west (Calvert & Ludden, 1999; Sénéchal et al., 1996). On the basis of this similarity, it is proposed that most faults associated reflectors relate to Neoarchean deformation (D_2, $\pm D_3$). Only a few apparent normal faults in area 3b (**Figure 6a**) could relate to doming or uplift associated with the Grenville orogeny (D_4) or to D_2-D_3 deformation (see below).

On the Chibougamau seismic profile, the most prominent reflectors are observed at the contact between supracrustal rocks of the upper-crust (zone A on **Figure 5b**) and the

mid-crust (zone B) regions. In other areas imaged by the Lithoprobe program, faults and shear zones tend to form stronger reflectors than do lithological contacts (Calvert & Ludden, 1999; Eaton et al., 2010; Snyder et al., 2008). The same may apply to the Chibougamau Metal Earth profile. The most prominent reflectors of the Chibougamau section are likely faults, and it is proposed that they obliterate a major lithological contact.

The upper to mid-crustal reflectors, on the Chibougamau profil, are imbricated and mostly dip toward the north. These anastomosed reflectors are located in an imbricated mid-crust area. Lithoprobe interpretations generalized structure of the mid-crust as a consequence of the N-S shortening event that led to terrane imbrication prio craton stabilization, with laterally extensive reflectors usually interpreted as crustal thrusts (Lacroix & Sawyer, 1995). A similar interpretation is postulated for the Chibougamau area, where most reflectors are likely reverse faults.

Reflective extensional structures were inferred in only a few areas in Lithoprobe interpretations (Calvert & Ludden, 1999). In the Chibougamau area, late extension is documented along the Barlow fault (Bedeaux et al., 2020) and postulated along some curved, intersecting reflectors observed in area 3b (**Figure 6a).** These structures may have accommodated the exhumation of parts of the crust, such as the gneisses of the Opatica plutonic belt to the north, toward the end of the main shortening event (D_2) or later (D_3). Faults associated with the reflectors of area 3b have offset geometries that can accommodate the exhumation of the part of the Obatogamau Formation located near the L2 marker (**Figure 7b**), explaining the relatively elevated metamorphic grade (upper greenschist to lower amphibolite facies) of these volcanic rocks compared to the rest of the Abitibi greenstone belt (Boucher et al., 2020).

In summary, north-dipping mid-crust reflectors likely mark faults that formed during imbrication of the Abitibi and Opatica crusts (**Figure 7**), during terrane assembly and cratonisation of the southern Superior craton (D_2 deformation event also referred to as the Kenoran orogeny), and shortening was followed by exhumation-related extension (D_3?). The listric faults and imbricated rock packages interpreted by the Lithoprobe program have been compared to the upper crust imbricated fan geometry observed in modern orogens (Lacroix & Sawyer, 1995). The Abitibi greenstone belt, however, differs from typical high-level thrust belts by the abundance of penetrative foliation, folds and ductile-brittle faults; it has a deeper and more ductile aspect (Lacroix & Sawyer, 1995). In the light of the new seismic data, such remarks also apply to the Chibougamau area.

4.3 Lithology of the crust

A difficulty that arises when interpreting seismic profiles of the crystalline crust is that reflectors may correspond to lithological contacts (layers, sills) or structures, including fluid-filled fractures (Lacroix & Sawyer, 1995), as well as contacts between rocks with different alteration styles or metamorphic grades (Eaton, 2006). For the Chibougamau area, the preferred interpretation is that most reflectors correspond to faults, and that these structures may obliterate lithological contacts (see previous section).

The lithology of the Chibougamau crust is interpreted using the Kapuskasing uplift as an analogue. This 500 km long uplift separates the Abitibi and Wawa subprovinces. The Kapuskasing uplift formed due to NE-directed crustal-scale thrust faulting (Percival & McGrath, 1986) during the Neoarchean (Duguet & Szumylo, 2016). This uplift exposes a section across the lower crust consisting of an upper sequence of supracrustal rocks cut by plutons (0 to <10 km thick), a middle sequence of gneissic batholiths with tonalite and granodiorite intrusions (< 10 to ~20 km), and a lower sequence (20 to >25 km) of granulite gneisses (Percival & Card, 1983; Percival & West, 1994).

The upper crust of the Chibougamau section (**Figure 5**) would correspond to supracrustal sequence of the Kapuskasing uplift, the mid-crust to intermediate to felsic intrusions and the lower crust to granulite facies gneisses. The uppermost part of the mid-crust is interpreted as a major lithological contact, with supracrustal rocks underlain by an intrusion-dominated zone (**Figures 7b, 7c**). The latter zone may contain numerous contacts between intrusions and supracrustal rocks superimposed by faults during deformation. The mid-crust may be exposed south of the study area, where the gneisses and foliated tonalite of the Hébert pluton crop out.

The Chibougamau profile also shows distinct mid- and lower-crust (**Figure 5b**). The mid- to lower-crust contact was imaged by many seismic profiles around the world, as it is a major metamorphic and/or compositional boundary (Salisbury & Fountain, 2012). This interpretation can be extended to the Chibougamau area, where the lower crust is likely made of granulite gneisses similar to those exposed in the Kapuskasing uplift. It remains unclear whether the lower crust evolved together with the mid and upper crust, or whether it corresponds to an older sialic basement.

In crustal cross-sections of convergent tectonic around the world, the crust-mantle transition tends to be blurred by large anorthosite bodies (Fountain & Salisbury, 1981; Salisbury & Fountain, 2012). This transition is not sharply defined in the Chibougamau area (**Figure 6b**). Given the abundance of mafic magmatism in the study area, this part of the crust could be composed of mafic to ultramafic bodies. Other magmatic bodies, as well as plagioclase- and amphibole-rich cumulates, may also occur at different levels in the crust; anorthosite-rich intrusions (e.g., Lac Doré Complex) are observed in the Chibougamau area and TTG suites are dominated by amphibole and plagioclase fractionation (Moyen & Martin, 2012). Below about 35 km depth, these mafic gneisses metamorphose into garnet-bearing granulites that have seismic properties indistinguishable from mantle peridotite or eclogite (Hynes & Snyder, 1995).

The Chibougamau R1 Metal Earth profile is also characterized by two 10-20 km wide attenuated areas (6a and 6b; **Figure 7**) interpreted as magmatic systems. These could also correspond to metasomatized regions that do not reach the surface, where no evidence of extensive alteration zones, or to hydrothermally altered rocks cross-cut by a large amount of magma intrusions, is observed.

Area 6b underlies the pluton alignment observed in the core of the La Dauversière anticline (**Figures 1, 7**), and these intrusions may correspond to the sub-surface expression of an extensive magmatic system. Area 6a, in contrast, underlays the Waconichi and Chibougamau synclines (marker L4; **Figure 7**). Large-volume plutons are located south (Chibougamau and Opémisca plutons) and north (Barlow pluton) of area 6a

(**Figure 7**), possibly because magma intrusions deviated within the upper crust (see next section). Area 6a may correspond to a long-lived magmatic system that operated during volcanic cycle 2 (Chibougamau pluton) or before, and was still active throughout the syntectonic period (Opémisca and Barlow plutons). Shortening-related faults formed in areas 6a and 6b were overprinted by magma intrusions, explaining the lack of prominent reflections in these areas.

4.4 Evolution of the crust

The oldest rocks exposed in the Chibougamau area are mafic and subordinate felsic volcanic rocks. During the synvolcanic period (starting at 2.80 Ga or before, and up to 2.73 Ga), the crust may have been mostly mafic. At the time of volcanic cycle 1 (**Figure 8a**), the mid- and lower-crust may have consisted of synvolcanic intrusions related to pre- and syn-Roy Group magmatism, or may correspond to an older crystalline basement (Chown & Mueller, 1992). Isotopic data however suggests that the Abitibi greenstone belt is mainly of juvenile character (W. J. Davis et al., 2000). This is more compatible with a continuous lower to upper crust that underwent a progressive maturation during TTG and subsequent magmatism. However, the Pilbara craton also has juvenile isotopic signatures, but it is underlain by older crust (Petersson et al., 2019). By analogy, an older crustal root for the Abitibi greenstone belt cannot be fully excluded. Solving how the mid- to lower-crust formed requires dedicated geochemical investigations that are beyond the scope of this paper, as seismic data cannot constrain the age of the crust.

The origin of the mafic crust of the Abitibi belt is also debated. In the Chibougamau area, mantle melts dominated volcanic cycle 1 (tholeiitic basalts, Lac Doré Complex) and continued during volcanic cycle 2 (Bruneau Formation, Cummings sills). There is no evidence for a depleted mantle source (i.e., no LILE- and LREE-depletion on the multi-element and REE diagrams), as is generally the case in Archean terranes (Moyen & Laurent, 2017). These types of magmas can be generated by modern plumes and similar plumes may have operated in the Archean and formed an oceanic plateau (Benn & Moyen, 2008). Alternatively, the basalts of the Abitibi greenstone belt may have formed by partial melting (30%) of the hot ambient upper mantle (Herzberg et al., 2010; Herzberg & Rudnick, 2012) and the Abitibi may represent a typical, >30 km thick, Archean oceanic crust. Both scenarios result in Abitibi crust that is initially thick and dominantly mafic (**Figure 8a**). It is postulated that the study area initiated as typical oceanic crust because the Chibougamau area lacks evidence of plume activity such as komatiite (Parman & Grove, 2005). This mafic crust was likely connected to older crust to the north (Opatica plutonic belt) as there is no evidence of obducted crust between the Abitibi and Opatica crusts (**Figure 8a**).

The Lac Doré Complex layered intrusion and associated VMS systems formed at about 2.73 Ga, during volcanic cycle 1. The volcanic architecture, at the time, either corresponded to plateau basalt or central shield volcano (**Figure 8a**). A part of the sedimentary rocks of the Caopatina Formation probably accumulated at this time, at the base of a volcano. Tonalite-dominated magmatism (i.e., TTG and TTD suites) may have initiated at this time or later, when thick mafic crust subducted and melted to produce TTG magmas (Martin et al., 2014). Although it is not easy to subduct an oceanic plateau,

there are modern examples in circum-Pacific (Bierlein & Pisarevsky, 2008). Alternatively, the thick mafic crust progressively evolved, through hydration, metamorphism and melting (to form TTG suites), toward a cratonic nucleus (Herzberg & Rudnick, 2012). Geochronological data are sparse in the Chibougamau area. At the time of writing, there is no evidence for pre-volcanic cycle 2 tonalite-dominated magmatism (**Figure 3**). Abundant partial melting of hydrated basalts located at depth may thus have initiated late, at or after 2.73 Ga, and ended at 2.71 Ga (**Figure 3**).

Tonalite-dominated intrusions are mostly exposed in the La Dauversière and Chibougamau anticlines (**Figure 1**). Little is known of the volcanic architecture during volcanic cycle 2 and we assume that a composite volcano was centered near marker L4, where most of the volcanic rocks of this period are exposed. Volcano load may then have controlled the location of magma intrusions, as had been shown experimentally (Kervyn et al., 2009; Mathieu, 2018; Mathieu & van Wyk de Vries, 2009). Intrusions may have been deviated toward the edge of the composite volcano to form the Chibougamau pluton, associated Cu-Au mineralization and, possibly, an overlaying secondary volcano (**Figure 8b**). The intrusions observed in the core of the La Dauversière anticline (Eau Jaune Complex, La Dauversière pluton) may be associated to a secondary magmatic system to the south (**Figure 8b**).

Intrusive activity likely domed supracrustal rocks, initiating the formation of the large-scale folds observed in the supracrustal rocks of the Chibougamau area (R. Daigneault & Allard, 1990). Deformation related to N-S shortening may also have initiated at the time to form reverse faults associated with prominent reflections in the mid-crust region. Imbrication with older crust to the north may have initiated at the time. Intense magmatic activity, during volcanic cycle 2, may then have obliterated the faults located in the area occupied by the main magmatic systems, i.e., areas 6a and 6b (**Figure 7**).

The main shortening event occurred during the syntectonic period (**Figure 8c**). Products from the erosion of cycle 2 volcano may have accumulated within depressions (synclines) north and south of marker L4 to form the Opémisca Group, and south of the La Dauversière anticline to form part of the Caopatina Formation. Progressive shortening has then tightened the anticlines centered on magma intrusions (see previous section) and imbricated the Abitibi and Opatica crusts (**Figure 7c**). Faults that accommodated doming and basin subsidence in the early stage of deformation may have been re-activated as reverse faults as the intensity of deformation increased.

To the north of the study area, the Barlow fault may then have accommodated normal motion, as exhumation of the Opatica plutonic belt progressed as a consequence of crustal imbrication (**Figure 8d**). Exhumation of the Hébert pluton, to the south of the study area, may be related to imbrication with additional crust to the south, as is observed elsewhere in the Abitibi greenstone belt (Bellefleur et al., 1995; Calvert & Ludden, 1999; Lacroix & Sawyer, 1995).

Syntectonic magmas may have infiltrated synvolcanic magmatic systems (areas 6a and 6b) to reach the surface, forming the Muscocho and other plutons in the La Dauversière anticline. Magma infiltrating area 6a has been deviated to the north (Barlow pluton) and south (Opémisca pluton), and has infiltrated at the apex of area 6a to form the

Chevrillon plutons and the numerous small-volume intrusions observed in the Waconichi tectonic zone (**Figure 1**), as it followed the major reverse and/or normal faults that were active at the time. Magmatism may highlight the main structures active at a given time (Mathieu et al., 2008, 2013) and, for this reason, it is proposed that the area located north of the Chibougamau city hosts the most active faults and magmatic systems, and possibly hydrothermal systems and related gold mineralization, of the syntectonic period (**Figure 8c, 8d**).

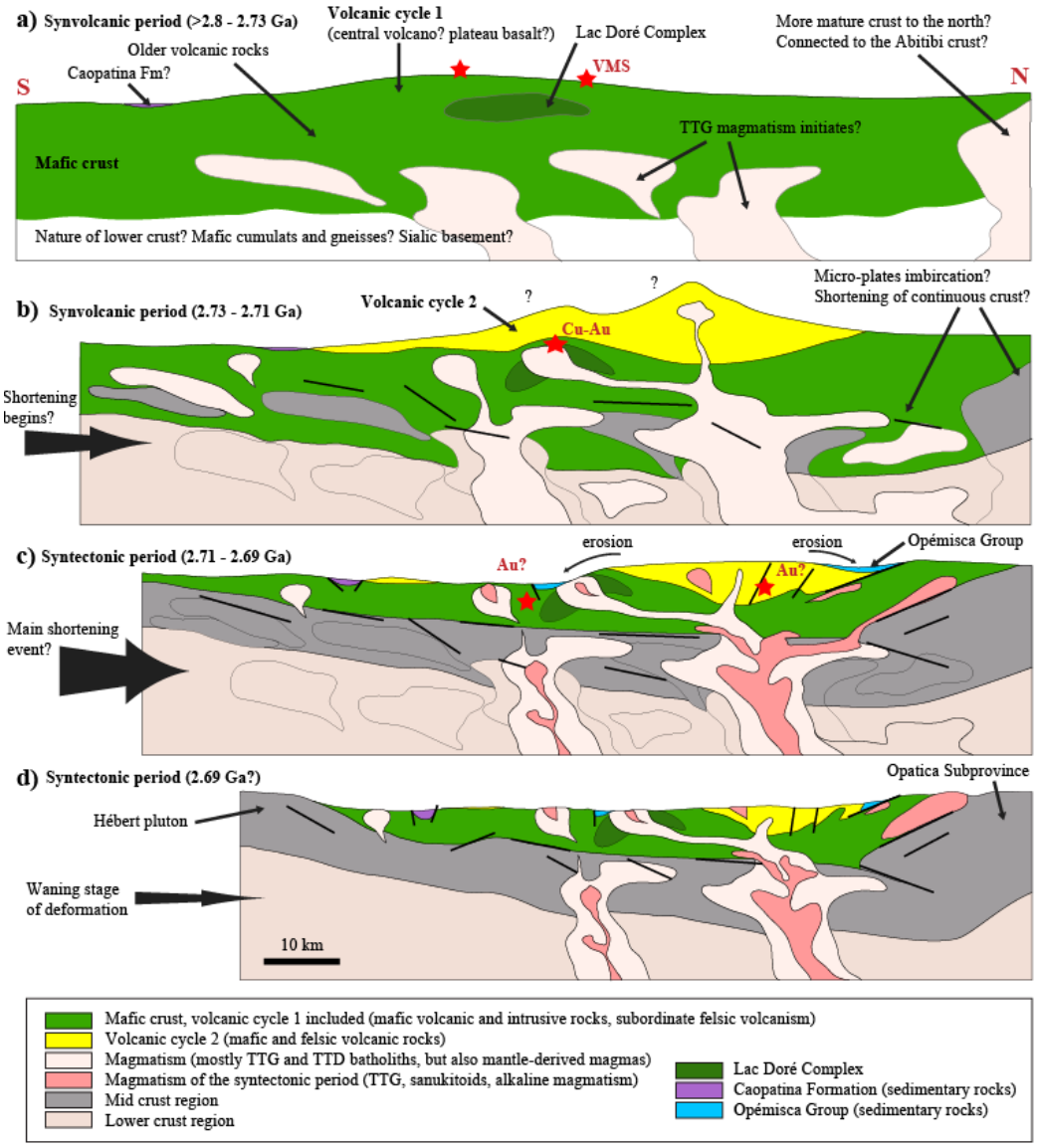

Figure 8. Evolution of the crust exposed in the Chibougamau area, between 2.80 Ga and 2.69 Ga (see text for explanation). The vertical scale for surface topography is arbitrary. The base of the diagram is located, from (a) to (d), at about 30 km depth (normal Archean oceanic crust) to >35 km depth toward the end of the shortening event, prior thinning related to post-Kenoran (?) and post-Grenville orogenies extension (present-day crust is 35 km thick in the study area). The mafic crust evolved into more felsic mid- and lower-crust through metamorphism, magma injections and local anatexis.

4.5 Geodynamic setting

The Abitibi greenstone belt represents juvenile and thickened lithospheric crust whose origin remains controversial. As postulated previously (Ludden & Hynes, 2000), the unique thermal regime of the Archean (Herzberg et al., 2010) may be one of the main factors that led to a crustal evolution distinct from what can be observed in modern geodynamic settings. In that sense, the notions of 'oceanic crust', 'subduction setting' and 'orogeny', among others, as we understand it today may not be directly applicable to the Archean.

The architecture of the southern Superior Province is interpreted on Lithoprobe seismic profiles in terms of imbricated terranes with large syn-accretionary faults and possibly fossil subduction zones that displaced the Moho. The Chibougamau area has also been interpreted by some as a volcanic island arc, which evolved from an immature oceanic arc to a mature arc crossed by multiple batholiths (Dimroth et al., 1985; Mueller et al., 1989). Other interpretations suggest that the exposed rocks represent a 10 km thick supracrustal sequence that was deposited on an older sialic crust of unknown origin (R. Daigneault & Allard, 1990) and that may be dominated by locally outcropping tonalitic gneisses, such as the Lapparent massif west of the Eau Jaune Complex (**Figure 1**) (Chown & Mueller, 1992). These interpretations reflect the prevalent view at the time of subduction-driven plate tectonics during the Archean (Clowes et al., 1998; Ludden & Hynes, 2000). Indeed, subduction can juxtapose lithologies of different provenances and structurally emplace supracrustal rocks deep beneath the crust (Fountain & Salisbury, 1981). However, as discussed in this section, geodynamic processes other than subduction may explain the reflectors on the Chibougamau seismic profile.

Archean geodynamic models may be divided into those that embrace the actualism principle and those that reject it. In other words, some models stipulate that ancient lithosphere behaved as today's stiff lithosphere, while others advocate for a much weaker lithosphere (Gapais et al., 2009; E Sizova et al., 2010). A subduction setting is the cornerstone of "actualistic" models, and these models typically invoke flatter subduction zones than those present today to explain the absence of a metasomatized mantle wedge in the Archean (Abbott et al., 1994; Chown et al., 1992; Kerrich & Polat, 2006). Other models stipulate that subduction tectonics began late, may be as late as the Neoproterozoic (Stern, 2005), and variants such as the 'hot subduction' model have been proposed for the Archean (Moyen & Laurent, 2018).

Assuming subduction-driven accretionary tectonics, the mid-crust region along the Chibougamau profile could be interpreted as Abitibi crust that was subducted northward beneath the Opatica crust. An additional northward-directed subduction beneath the study area is required to emplace hydrated basalts beneath the Chibougamau area to produce TTG melts. There is evidence of mid-crustal imbrication in the northern part of the seismic profile (**Figure 5**) but there is no evidence for a slab subducted beneath the study area. The study area also lacks typical 'arc magma'; i.e., mafic magma with calc-alkaline affinity derived from the hydrous melting of a mantle wedge. The only volcanic rocks with calc-alkaline affinities are intermediate to felsic in composition. By analogy with modern settings (Blum Oeste & Wörner, 2016; Wörner et al., 2018), these rocks may be crustal melts (hydrated basaltic source), with anatexis induced by the emplacement of mantle-derived magmas in the crust. Anatexis of the crust formed felsic melts that more

or less hybridized with mafic mantle-derived melts to produce intermediate melts (Bédard, 2018). We argue that no evidence supports a modern-style subduction process in the Chibougamau area.

Other geodynamic models for the Archean period invoke mantle plume activity as the driving factor in the formation of Archean crust (Gerya et al., 2015). Superplume activity may have led to peak juvenile crust production at 2.75 Ga (Mints, 2017). Part of the crust may then have locally evolved (e.g., Abitibi area) within a subduction setting (Mints, 2017). The partial convective overturn model alternates between horizontal motions (plate tectonics) and stages of mantle plume-driven crustal reworking (Rey et al., 2003). The Archean subcretion model also invokes horizontal movement followed by the imbrication of crust that is too thick to subduct and that matures, melts and produces TTG magmas (Bédard, 2018; Bedard et al., 2013; Bédard et al., 2003). Another category of model stipulates that vertical movement dominates and that the crust and upper mantle were re-worked through convection, sinking of dense greenstone belts or diapir-type gravitational instabilities, i.e., sagduction (Chardon et al., 1996; François et al., 2014; Van Kranendonk, 2011; Lin et al., 2013; Van Thienen et al., 2004). No evidence of vertically 'dripping' mafic rock packages is observed on the Chibougamau seismic profile, and the sagduction model may apply better to greenstone belts with components older than the juvenile Abitibi belt.

Most of these models stipulate that TTG magmatism comes from the progressive maturation of the crust. Tonalites of TTG suites originate from partial melting of hydrated and metamorphosed enriched-basalts (Martin et al., 2014). The chemistry of TTG suites (HREE depletion, high Al-content) has indeed long been interpreted as the result of partial melting of hydrated basalts at depth, within the stability field of amphibole and garnet (Moyen & Martin, 2012). Subduction can introduce mafic rocks to a deep environment (Moyen & Laurent, 2018), as can delamination (Bédard, 2018; Bedard et al., 2013; Elena Sizova et al., 2015), while melting of the base of a thickened crust is another possibility (Van Kranendonk et al., 2015). A matter raised by the latter models is whether basalts hydrated by sea water can be buried fast enough to produce the H_2O-rich source of the TTG suite. Another matter that remains to be investigated is whether tonalites are HREE-depleted because they come from the melting of a basaltic source in the stability field of garnet (Moyen & Martin, 2012) or whether the HREE-depletion is mostly due to differentiation controlled by amphibole and apatite (Liou & Guo, 2019).

In the light of these geodynamic models and considering the lack of komatiite in the study area, we propose that the study area initiated as a normal Archean oceanic crust; i.e., as a thickened and dominantly mafic crust that formed at about, or before, 2.80 Ga (**Table 1, Figure 3**). Mantle-derived melts formed most of the crust, while the more felsic so-called "calc-alkaline" volcanic rocks can be explained by anatexis induced by the accumulation of mantle-derived melts in the mafic crust. We propose that shortening induced imbrication with older crust to the north, forming the mid-crustal imbrication observed on the seismic profile (**Figure 7b**). The imbrication induced rapid burial of hydrated mafic rocks, which may have rapidly de-hydrated to produce a 'pulse' of TTG magmatism during volcanic cycle 2, and that this pulse lasted no longer than 20 Myr. Other magmas (e.g., intermediate volcanic rocks, diorite of the TTD suites) may be

915 explained by mixing between mantle-derived and TTG melts (Mathieu et al., 2020),
916 implying that partial melting of mantle rocks continued but declined during volcanic
917 cycle 2. This model implies that shortening, as well as imbrication between the Abitibi
918 and Opatica crusts, started during the synvolcanic period and continued throughout the
919 syntectonic period (so-called Kenoran orogeny). This formed faults and folds in the
920 upper- and mid-crustal regions (**Figure 7**), while magmatic activity declined.

921

922 **4.6 Metallogenic implications**

923 The preliminary geodynamic model proposed in the previous section has several
924 metallogenic implications. In the Chibougamau area, the main VMS mineralization is
925 associated with the Waconichi Formation. Sea-floor mineralizing processes may have
926 been favored by a decrease in the eruption rate, as the geodynamic setting evolved from
927 oceanic (plateau basalt or typical Archean oceanic crust) to collisional. The VMS systems
928 cluster around a major heat source, i.e., the Lac Doré Complex, which is equivalent to the
929 Bell River Complex of the Matagami mining camp (Piche et al., 1993). Seismic data
930 show no major difference between the structure of the crust of the Chibougamau and
931 Matagami areas. The Chibougamau area is not, however, renowned for its VMS deposits,
932 the Lemoine deposit excepted (Mercier-Langevin et al., 2014). There may be significant
933 differences in the extent, efficiency and duration of both hydrothermal systems that
934 cannot be explained by geodynamic context differences and that should be investigated
935 by dedicated studies.

936 Chibougamau is however a Cu-Au mining camp known for its magmatic-
937 hydrothermal deposits centered on the Chibougamau pluton (P Pilote et al., 1997). The
938 imbrication of parts of the oceanic crust followed by rapid devolatilization and melting of
939 mafic rocks to produce TTG suites, and possible mixing with mantle-derived melt to
940 produce TTD, all seem favorable to the production of Cu-Au-bearing hydrous magmas.
941 Magmas able to contribute fluids and metals to mineralizing systems also formed during
942 the syntectonic period, e.g., MOP-II (Lépine, 2009) and Lac Line (Côté-Mantha, 2009)
943 polymetallic mineralization. The lithosphere of the Chibougamau area seems particularly
944 favorable to magmatic-hydrothermal systems. This is either due to abnormal abundance
945 of sulfur and metals in the deep parts of the crust or underlying mantle rocks, or to
946 favorable processes, such as intrusions emplaced at depths favorable for fluid exsolution
947 and the initiation of hydrothermal processes.

948 Continued shortening during terrane imbrication caused additional burial and
949 metamorphic devolatilization, producing fluids that induced orogenic gold-style of
950 mineralization in the Chibougamau area (Leclerc et al., 2017). However, the
951 Chibougamau area historically had minor gold production and few economic deposits
952 have been discovered, possibly because no crustal-scale sub-vertical fault system
953 comparable to the Cadillac-Larder Lake fault of southern Abitibi (Bedeaux et al., 2018)
954 has efficiently channeled these fluids. Alternatively, an abundant source for Au, such as
955 the Pontiac sedimentary subprovince (Pitcairn & Leventis, 2017), is lacking in the
956 Chibougamau area. The supracrustal succession (potential source rocks) is thickest north
957 of the town of Chibougamau, where the Waconichi tectonic zone is observed. According
958 to the data presented here, this structure has channelized numerous small-volume

959 syntectonic intrusions and has accommodated a significant amount of displacement. This
960 could be the most prospective domain for gold mineralization.

961

962 **5 Conclusions**

963 This contribution presents the first seismic reflection profiling of the Chibougamau
964 area, located in the northeastern corner of the Neoarchean Abitibi greenstone belt. The
965 Chibougamau area shares many similarities with the Matagami area to the west, studied
966 by the Lithoprobe program in the 1990s, suggesting that the northern part of the Abitibi
967 belt has a consistent structure and a uniform geodynamic evolution. Combining new
968 seismic data with the known stratigraphy, structure and magmatic records of the
969 Chibougamau area, we propose that it represents normal Archean oceanic crust that
970 evolved through imbrication and collision with an older crustal block located to the north.
971 Subduction and other post-Proterozoic geodynamic settings unlikely apply to the
972 Neoarchean period. This contribution proposes that the structure and magmatic systems
973 of the Chibougamau crust result from horizontal shortening that induced terrane
974 imbrication in a fashion that differs from modern-day subduction and collisional
975 processes. Terrane imbrication induced rapid burial, devolatilization, and partial melting
976 of the mafic crust, giving raise to tonalite-dominated magmatism (TTG suite) and
977 granulite-facies metamorphic rocks below 35 km depth. Possible hybridization between
978 TTG and mantle-derived melts gave rise to the TTD suite and associated Cu-Au
979 magmatic-hydrothermal mineralization. Continued devolatilization metasomatized parts
980 of the crust and provided conditions that would have been favorable to the development
981 of orogenic gold-style of mineralization. However, the paucity of economic Au deposits
982 in the Chibougamau area likely reflects the absence of major transcrustal fault systems
983 similar to those observed in the southern part of the Abitibi greenstone belt.

984

985 **Acknowledgments**

986 Many thanks to Editor J. Geissman and to two anonymous reviewers, who greatly
987 contributed to improve the quality of this manuscript. Warm thanks are addressed to
988 SAExploration, for seismic data acquisition, and to Absolute Imaging Inc. for initial
989 processing. Prof. E.W. Sawyer, UQAC University, is also thanked for critically
990 reviewing an early version of this contribution. This study was undertaken as part of the
991 Metal Earth project (Laurentian University) investigation of the Chibougamau area, and
992 this research was funded by Canada First Research Excellence Funds and by
993 federal/provincial/industry partners (http://merc.laurentian.ca/research/metal-earth/). This
994 paper is Metal Earth contribution number MERC-ME-2020-002.

995 Data availability: Archiving of the Metal Earth R1 seismic profile of the Chibougamau
996 area (**Figure 5a**) in the Snolab repository is underway. This data is also available as
997 supporting information to this contribution.

998

999 **Supporting information**

The following are available online: Supporting information S1.pdf—contains migrated Chibougamau R1 profile (full view and zooms), as well as amplitude versus frequency graphics; Supporting information S2.pdf—migrated Chibougamau R1 profile (an moderate coherency filter has been applied); Supporting information S3.pdf—migrated Chibougamau R1 profile (an intense coherency filter has been applied); Supporting information S4.pdf—alternative interpretations of the Chibougamau seismic profile.

References

Abbott, D., Drury, R., & Smith, W. H. F. (1994). Flat to steep transition in subduction style. *Geology*, *22*(10), 937–940.

Adam, E., Milkereit, B., & Mareschal, M. (1998). Seismic reflection and borehole geophysical investigations in the Matagami mining camp. *Canadian Journal of Earth Sciences*, *35*(6), 686–695.

Allard, G. O. (1976). *Doré Lake Complex and its importance to Chibougamau Geology and Metallogeny*. MRN report DPV-386, Ministère des Ressources Naturelles: Québec, QC, Canada.

Archer, P. (1983). *Interpretation de l'environnement volcano-sédimentaire de la formation de Blondeau dans la section stratigraphique du lac Barlow, Chibougamau*. Unpublished Master thesis, Université du Québec à Chicoutimi, Chicoutimi, QC, Canada.

Ayer, J. A., Thurston, P. C., & Lafrance, B. (2008). A special issue devoted to base metal and gold metallogeny at regional, camp, and deposit scales in the Abitibi greenstone belt: Preface. *Economic Geology*, *103*(6), 1091–1096.

Baker, D. J. (1980). *The metamorphism and structural history of the Grenville Front near Chibougamau; unpub*. Unpublished PhD thesis, University of Georigia, Athens, GA, United-States.

Le Bas, M. J., Le Maitre, R. W., & Woolley, A. R. (1992). The construction of the total alkali-silica chemical classification of volcanic rocks. *Mineralogy and Petrology*, *46*(1), 1–22. https://doi.org/10.1007/BF01160698

Bedard, J. H., Harris, L. B., & Thurston, P. C. (2013). The hunting of the snArc. *Precambrian Research*, *229*, 20–48.

Bédard, J. H. (2018). Stagnant lids and mantle overturns: Implications for Archaean tectonics, magmagenesis, crustal growth, mantle evolution, and the start of plate tectonics. *Geoscience Frontiers*, *9*(1), 19–49.

Bédard, J. H., Brouillette, P., Madore, L., & Berclaz, A. (2003). Archaean cratonization and deformation in the northern Superior Province, Canada: an evaluation of plate tectonic versus vertical tectonic models. *Precambrian Research*, *127*(1–3), 61–87.

Bédard, J. H., Leclerc, F., Harris, L. B., & Goulet, N. (2009). Intra-sill magmatic evolution in the Cummings Complex, Abitibi greenstone belt: Tholeiitic to calc-alkaline magmatism recorded in an Archaean subvolcanic conduit system. *Lithos*, *111*(1), 47–71.

Bedeaux, P., Mathieu, L., Pilote, P., Rafini, S., & Daigneault, R. (2018). Origin of the Piché Structural Complex and implications for the early evolution of the Archean crustal-scale Cadillac-Larder Lake Fault Zone, Canada. *Canadian Journal of Earth Sciences*, *55*(8), 905–922.

Bedeaux, P., Brochu, A., Mathieu, L., Gaboury, D., & Daigneault, R. (2020). Gold endowment of the Barlow Fault, Chibougamau area, Neoarchean Abitibi subprovince: insight from structural analysis and metamorphism. *Canadian Journal of Earth Sciences, submitted*.

Bellefleur, G., Barnes, A., Calvert, A., Hubert, C., & Mareschal, M. (1995). Seismic reflection constraints from Lithoprobe line 29 on the upper crustal structure of the northern Abitibi greenstone belt. *Canadian Journal of Earth Sciences*, *32*(2), 128–134.

Benn, K., & Moyen, J.-F. (2008). The Late Archean Abitibi-Opatica terrane, Superior Province: A modi ed oceanic plateau. *When Did Plate Tectonics Begin on Planet Earth?*, *440*, 173.

Bierlein, F. P., & Pisarevsky, S. (2008). Plume-related oceanic plateaus as a potential source of gold mineralization. *Economic Geology*, *103*(2), 425–430.

Blum Oeste, M., & Wörner, G. (2016). Central Andean magmatism can be constrained by three ubiquitous end members. *Terra Nova*, *28*(6), 434–440.

Boucher, A., Mathieu, L., Hamilton, M., Bedeaux, P., & Daigneault, R. (2020). Petrogenesis and economic potential of the Obatogamau Formation, Chibougamau area, Abitibi Subprovince. *Canadian Journal of Earth Sciences, submitted*.

Calvert, A. J., & Ludden, J. N. (1999). Archean continental assembly in the southeastern Superior Province of Canada. *Tectonics*, *18*(3), 412–429.

Caty, J.-L. (1975). *Géologie de la demie ouest du canton de Richardson (comté d'Abitibi-Est)*. MRN report DP 342, 2 maps; Ministère des Richesses Naturelles: Québec, QC, Canada.

Caty, J.-L. (1978). *Canton de Richardson (comté d'Abitibi-Est)*. MRN report DP 606. 1 map; Ministère des Ressources Naturelles: Québec, QC, Canada.

Caty, J.-L. (1979). *Géologie de la demie ouest du canton de Bignell*. MRN report DPV 678, 1 map; Ministère des Ressources Naturelles: Québec, QC, Canada.

Chardon, D., Choukroune, P., & Jayananda, M. (1996). Strain patterns, décollement and incipient sagducted greenstone terrains in the Archaean Dharwar craton (south India). *Journal of Structural Geology*, *18*(8), 991–1004.

Cheraghi, S., Naghizadeh, M., Snyder, D., & Mathieu, L. (2018). Crustal-scale seismic investigation in Chibougamau, Quebec, Canada. In *Near Surface Geoscience 2018 (EAGE), Workshop: worldwide Mineral Exploration Challenges and Cost-effective Geophysical Methods, Porto, Portugal. Abstract*.

Cheraghi, S., Naghizadeh, M., Snyder, D., Haugaard, R., & Gemmell, T. (2019). High resolution seismic imaging of crooked two dimensional profiles in greenstone belts of the Canadian shield: results from the Swayze area, Ontario, Canada. *Geophysical*

Prospecting.

Chown, E. H., & Mueller, W. U. (1992). Basement influence on the supracrustal and plutonic deformation of an Archean Greenstone Belt. In R. Mason (Ed.), *International Basement Tectonics Association* (pp. 465–476). Publication No. 7, Kluwer Academic Publishers, Dordrecht.

Chown, E. H., Daigneault, R., Mueller, W., & Mortensen, J. K. (1992). Tectonic evolution of the northern volcanic zone, Abitibi belt, Quebec. *Canadian Journal of Earth Sciences*, *29*(10), 2211–2225.

Clowes, R. M., Cook, F. A., & Ludden, J. N. (1998). Lithoprobe leads to new perspectives on continental evolution. *Gsa Today*, *8*(10), 1–7.

Côté-Mantha, O. (2009). *Architecture et origine du système de minéralisation polymétallique du secteur Lac Line, région de Chibougamau, Québec*. Unpublished PhD thesis, Université du Québec à Chicoutimi, Chicoutimi, QC, Canada.

Daigneault, R., & Allard, G. O. (1990). *Le Complexe du lac Doré et son environnement géologique (région de Chibougamau-sous-province de l'Abitibi)*. MRN report MM-89-03, Ministère des Ressources Naturelles: Québec, QC, Canada.

Daigneault, R, St-Julien, P., & Allard, G. O. (1990). Tectonic evolution of the northeast portion of the Archean Abitibi greenstone belt, Chibougamau area, Quebec. *Canadian Journal of Earth Sciences*, *27*(12), 1714–1736.

Daigneault, Réal. (1996). *Couloirs de déformation de al Sous-Province de l'Abitibi*. MRN report MB-96-33, Ministère des ressources naturelles: Québec, QC, Canada.

Dallmeyer, R. D., Maybin, A. H., & Durocher, M. E. (1975). Timing of Kenoran Metamorphism in the Eastern Abitibi Greenstone Belt, Quebec: Evidence From 40Ar/39Ar Ages of Hornblende and Biotite From Post-Kinematic Plutons. *Canadian Journal of Earth Sciences*, *12*(11), 1864–1873.

David, J., Dion, C., Goutier, J., Roy, P., Bandyayera, D., Legault, M., & Rhéaume, P. (2006). *Datations U-Pb Effectuées dans la Sous-province de l'Abitibi à la suite des travaux de 2004-2005*. MRN report RP 2006-04; Ministère des Ressources Naturelles et de la Faune: Québec, QC, Canada.

David, J., Davis, D. W., Dion, C., Goutier, J., Legault, M., & Roy, P. (2007). *Datations U-Pb Effectuées dans la Sous-province de l'Abitibi en 2005-2006*. MRN report RP 2007-01; Ministère des Ressources Naturelles: Québec, QC, Canada.

David, J., Vaillancourt, D., Bandyayera, D., Simard, M., Goutier, J., Pilote, P., et al. (2011). *Datations U-Pb Effectuées dans les Sousprovinces d'Ashuanipi, de La Grande, d'Opinaca et d'Abitibi en 2008-2009*. MERN report, RP-2010-11; Ministère de l'Énergie et des Ressources Naturelles: Québec, QC, Canada.

Davis, D., Simard, M., Hammouche, H., Bandyayera, D., Goutier, J., Pilote, P., et al. (2014). *Datations U-Pb Effectuées dans les Provinces du Supérieur et de Churchill en 2011-2012*. MERN report RP-2014-05; Ministère de l'Énergie et des Ressources Naturelles: Québec, QC, Canada.

Davis, W. J., Machado, N., Gariépy, C., Sawyer, E. W., & Benn, K. (1995). U-Pb

geochronology of the Opatica tonalite-gneiss belt and its relationship to the Abitibi greenstone belt, Superior Province, Quebec. *Canadian Journal of Earth Sciences*, *32*(2), 113–127.

Davis, W. J., Lacroix, S., Gariépy, C., & Machado, N. (2000). Geochronology and radiogenic isotope geochemistry of plutonic rocks from the central Abitibi subprovince: significance to the internal subdivision and plutono-tectonic evolution of the Abitibi belt. *Canadian Journal of Earth Sciences*, *37*(2–3), 117–133.

Dembele, Y. (1984). *Interprétation géochimique de l'environnement volcano-sédimentaire de la formation de Blondeau dans la section stratigraphique Cuvier-Barlow, Chibougamau*. Unpublished Master thesis, Université du Québec à Chicoutimi, Chicoutimi, QC, Canada.

Dimroth, E., Imreh, L., Goulet, N., & Rocheleau, M. (1983). Evolution of the south-central segment of the Archean Abitibi Belt, Quebec. Part III: Plutonic and metamorphic evolution and geotectonic model. *Canadian Journal of Earth Sciences*, *20*(9), 1374–1388.

Dimroth, E., Rochelau, M., Mueller, W., Archer, P., Brisson, H., Fortin, G., et al. (1985). Paleogeographic and paleotectonic response to magmatic processes: a case history from the Archean sequence in the Chibougamau area, Quebec. *Geologische Rundschau*, *74*(1), 11–32.

Dimroth, E., Mueller, W., Daigneault, R., Brisson, H., Poitras, A., & Rocheleau, M. (1986). Diapirism during regional compression: the structural pattern in the Chibougamau region of the Archean Abitibi Belt, Quebec. *Geologische Rundschau*, *75*(3), 715–736.

Dubé, B. (1990). *Métallogénie aurifère du fi lon-couche de Bourbeau, région de Chibougamau, Québec*. Unpublished PhD thesis, Université du Québec à Chicoutimi, Chicoutimi, QC, Canada.

Dubé, B., & Gosselin, P. (2007). Greenstone-hosted quartz-carbonate vein deposits. *Geological Association of Canada, Mineral Deposits Division*, 49–73.

Dubé, B., & Guha, J. (1987). *Étude métallogénique du filon-couche de Bourbeau. Les indices aurifères – région de Chibougamau*. MRN report MB 87-03; Ministère des Ressources Naturelles: Québec, QC, Canada.

Duguet, M., & Szumylo, N. (2016). Project NE-16-002. Archean and Proterozoic geology of the Borden Lake area, Kapuskasing structural zone, Abitibi-Wawa terrane. In *Summary of Field Work and Other Activities, 2016* (pp. 4–1 to 4–20). Ontario Geological Survey, Open File Report 6323.

Duquette, G. (1964). *Géologie du quart nord-ouest du canton de Roy, comté d'Abitibi-Est*. MRN report RP 513; Ministère des Ressources Naturelles: Québec, QC, Canada.

Duquette, G. (1982). *Demie nord des cantons de McKenzie et de Roy et quart nord-ouest du canton de McCorkill*. MRN report DPV 837, 4 maps; Ministère des Ressources Naturelles: Québec, QC, Canada.

Eaton, D. W. (2006). Multi genetic origin of the continental Moho: Insights from Lithoprobe. *Terra Nova*, *18*(1), 34–43.

Eaton, D. W., Adam, E., Milkereit, B., Salisbury, M., Roberts, B., White, D., & Wright, J. (2010). Enhancing base-metal exploration with seismic imagingThis article is one of a series of papers published in this Special Issue on the theme Lithoprobe-parameters, processes, and the evolution of a continent. *Canadian Journal of Earth Sciences*, *47*(5), 741–760.

Faure, S. (2015). *Relations entre les minéralisations aurifères et les isogrades métamorphiques en Abitibi / Relationship between gold mineralisations and metamorphic isograde in Abitibi [online]*. Consorem project 2013-03, available at: http://www.consorem.ca/rapports_publics.html (accessed on 10th of august 2018).

Fountain, D. M., & Salisbury, M. H. (1981). Exposed cross-sections through the continental crust: implications for crustal structure, petrology, and evolution. *Earth and Planetary Science Letters*, *56*, 263–277.

François, C., Philippot, P., Rey, P., & Rubatto, D. (2014). Burial and exhumation during Archean sagduction in the East Pilbara granite-greenstone terrane. *Earth and Planetary Science Letters*, *396*, 235–251.

Galland, O., De Bremond d'Ars, J., Cobbold, P. R., & Hallot, E. (2003). Physical models of magmatic intrusion during thrusting. *Terra Nova*, *15*(6), 405–409.

Gapais, D., Cagnard, F., Gueydan, F., Barbey, P., & Ballevre, M. (2009). Mountain building and exhumation processes through time: inferences from nature and models. *Terra Nova*, *21*(3), 188–194.

Gerya, T., Stern, R. J., Baes, M., Fischer, R., Sizova, E., Sobolev, S. V, & Whattam, S. A. (2015). Plume tectonics and cratons formation in the early Earth. In *AGU Fall Meeting Abstracts*.

Gosselin, P., & Dubé, B. (2005). *Gold deposits of the world: distribution, geological parameters and gold content*. Geological Survey of Canada Open File 4895.

Hamid, G. (1993). *Étude de la géométrie et des mouvements de la faille de Doda (sous-province de l'Abitibi)*. Unpublished Master thesis thesis, Université du Québec à Chicoutimi, Chicoutimi, QC, Canada.

Heinson, G., Didana, Y., Soeffky, P., Thiel, S., & Wise, T. (2018). The crustal geophysical signature of a world-class magmatic mineral system. *Scientific Reports*, *8*(1), 1–6.

Herzberg, C., & Rudnick, R. (2012). Formation of cratonic lithosphere: an integrated thermal and petrological model. *Lithos*, *149*, 4–15.

Herzberg, C., Condie, K., & Korenaga, J. (2010). Thermal history of the Earth and its petrological expression. *Earth and Planetary Science Letters*, *292*(1–2), 79–88.

Hynes, A., & Snyder, D. B. (1995). Deep-crustal mineral assemblages and potential for crustal rocks below the Moho in the Scottish Caledonides. *Geophysical Journal International*, *123*(2), 323–339.

Irvine, T. N. J., & Baragar, W. (1971). A guide to the chemical classification of the common volcanic rocks. *Canadian Journal of Earth Sciences*, *8*(5), 523–548.

Jolly, W. T. (1974). Regional metamorphic zonation as an aid in study of Archean terrains: Abitibi region, Ontario. *Canadian Mineralogist*, *12*, 499–508.

Kerrich, R., & Polat, A. (2006). Archean greenstone-tonalite duality: thermochemical mantle convection models or plate tectonics in the early Earth global dynamics? *Tectonophysics*, *415*(1–4), 141–165.

Kervyn, M., Ernst, G. G. J., van Wyk de Vries, B., Mathieu, L., & Jacobs, P. (2009). Volcano load control on dyke propagation and vent distribution: Insights from analogue modeling. *Journal of Geophysical Research*, *114*(B3), 26. https://doi.org/10.1029/2008JB005653

Khazanehdari, J., Rutter, E. H., & Brodie, K. H. (2000). High pressure high temperature seismic velocity structure of the midcrustal and lower crustal rocks of the Ivrea Verbano zone and Serie dei Laghi, NW Italy. *Journal of Geophysical Research: Solid Earth*, *105*(B6), 13843–13858.

Kline, S. W. (1985). *Metamorphic mineral chemistry, petrology, and sulfide mineralogy of the Dore Lake complex, Chibougamau, Quebec*. Unpublished PhD thesis, University of Georgia, Athens, GA, USA.

Van Kranendonk, M. J. (2011). Cool greenstone drips and the role of partial convective overturn in Barberton greenstone belt evolution. *Journal of African Earth Sciences*, *60*(5), 346–352.

Van Kranendonk, M. J., Smithies, R. H., Griffin, W. L., Huston, D. L., Hickman, A. H., Champion, D. C., et al. (2015). Making it thick: a volcanic plateau origin of Palaeoarchean continental lithosphere of the Pilbara and Kaapvaal cratons. *Geological Society, London, Special Publications*, *389*(1), 83–111.

Lacroix, S., & Sawyer, E. W. (1995). An Archean fold-thrust belt in the northwestern Abitibi Greenstone Belt: structural and seismic evidence. *Canadian Journal of Earth Sciences*, *32*(2), 97–112.

Laurent, O., Martin, H., Moyen, J.-F., & Doucelance, R. (2014). The diversity and evolution of late-Archean granitoids: Evidence for the onset of "modern-style" plate tectonics between 3.0 and 2.5 Ga. *Lithos*, *205*, 208–235.

Leclerc, F., Bédard, J. H., Harris, L. B., McNicoll, V. J., Goulet, N., Roy, P., & Houle, P. (2011). Tholeiitic to calc-alkaline cyclic volcanism in the Roy Group, Chibougamau area, Abitibi Greenstone Belt—revised stratigraphy and implications for VHMS exploration. *Canadian Journal of Earth Sciences*, *48*(3), 661–694.

Leclerc, F., Harris, L. B., Bédard, J. H., van Breemen, O., & Goulet, N. (2012). Structural and Stratigraphic Controls on Magmatic, Volcanogenic, and Shear Zone-Hosted Mineralization in the Chapais-Chibougamau Mining Camp, Northeastern Abitibi, Canada. *Economic Geology*, *107*(5), 963–989.

Leclerc, F., Roy, P., Pilote, P., Bédard, J. H., Harris, L. B., McNicoll, V. J., et al. (2017). *Géologie de la Région de Chibougamau*. MERN report RG 2015-03, Ministère de

l'Énergie et des Ressources Naturelles: Québec, QC, Canada.

Lefebvre, C. (1991). *Étude de la genèse des pépérites et de leur contexte volcano-sédimentaire, formation de Blondeau, Chibougamau, Québec*. Unpublished Master thesis, McGill University, Montréal, QC, Canada.

Legault, M. I. (2003). *Environnement métallogénique du couloir de Fancamp avec emphase sur les gisements aurifères de Chevrier, région de Chibougamau, Québec*. Université du Québec à Chicoutimi.

Lépine, S. (2009). *Le gîte à Au-Cu-Mo de MOP-II (Chibougamau, Québec) : un porphyre archéen déformé*. Unpublished Master thesis, Université du Québec à Montréal, Montréal, QC, Canada.

Lin, S., Parks, J., Heaman, L. M., Simonetti, A., & Corkery, M. T. (2013). Diapirism and sagduction as a mechanism for deposition and burial of "Timiskaming-type" sedimentary sequences, Superior Province: Evidence from detrital zircon geochronology and implications for the Borden Lake conglomerate in the exposed middle to lower. *Precambrian Research*, *238*, 148–157.

Liou, P., & Guo, J. (2019). Generation of Archaean TTG Gneisses Through Amphibole Dominated Fractionation. *Journal of Geophysical Research: Solid Earth*, *124*(4), 3605–3619.

Ludden, J., & Hynes, A. (2000). The Lithoprobe Abitibi-Grenville transect: two billion years of crust formation and recycling in the Precambrian Shield of Canada. *Canadian Journal of Earth Sciences*, *37*(2–3), 459–476.

Ludden, J., Hubert, C., Barnes, A., Milkereit, B., & Sawyer, E. (1993). A three dimensional perspective on the evolution of Archaean crust: LITHOPROBE seismic reflection images in the southwestern Superior Province. *Lithos*, *30*(3–4), 357–372.

Maleki Ghahfarokhi, A. (2019). *Gravity data acquisition and potential-field data modelling along Metal Earth's Chibougamau transect using geophysical and geological constraints*. Unpublished Master thesis, University of Laurentia, Sudbury, ON, Canada.

Martignole, J., & Calvert, A. J. (1996). Crustal scale shortening and extension across the Grenville province of western Quebec. *Tectonics*, *15*(2), 376–386.

Martin, H., Moyen, J.-F., Guitreau, M., Blichert-Toft, J., & Le Pennec, J.-L. (2014). Why Archaean TTG cannot be generated by MORB melting in subduction zones. *Lithos*, *198*, 1–13.

Mathieu, L. (2018). The structure of composite volcanoes unravelled by analogue modeling: A review. *Journal of Structural Geology*.

Mathieu, L. (2019). Origin of the Vanadiferous Serpentine-Magnetite Rocks of the Mt. Sorcerer Area, Lac Doré Layered Intrusion, Chibougamau, Québec. *Geosciences*, *9*(3), 110.

Mathieu, L., & Racicot, D. (2019). Petrogenetic Study of the Multiphase Chibougamau Pluton: Archaean Magmas Associated with Cu-Au Magmato-Hydrothermal Systems. *Minerals*, *9*(3), 174.

Mathieu, L., & van Wyk de Vries, B. (2009). Edifice and substrata deformation induced by intrusive complexes and gravitational loading in the Mull volcano (Scotland). *Bulletin of Volcanology*, *71*(10). https://doi.org/10.1007/s00445-009-0295-5

Mathieu, L., van Wyk de Vries, B., Holohan, E. P., & Troll, V. R. (2008). Dykes, cups, saucers and sills: Analogue experiments on magma intrusion into brittle rocks. *Earth and Planetary Science Letters*, *271*(1–4). https://doi.org/10.1016/j.epsl.2008.02.020

Mathieu, L., van Wyk de Vries, B., Mannessiez, C., Mazzoni, N., Savry, C., & Troll, V. R. (2013). The structure and morphology of the Basse Terre Island, Lesser Antilles volcanic arc. *Bulletin of Volcanology*, *75*(3), 1–15. https://doi.org/10.1007/s00445-013-0700-y

Mathieu, L., Crépon, A., & Kontak, D. J. (2020). Tonalite-Dominated Magmatism in the Abitibi Subprovince, Canada, and Significance for Cu-Au Magmatic-Hydrothermal Systems. *Minerals*, *10*(3), 242.

McMillan, R. H. (1972). *Petrology, geochemistry and wallrock alteration at Opemiska – A vein copper deposit crosscutting a layered Archean ultramafi c sill*. Unpublished PhD thesis, Western University, London, ON, Canada.

Mercier-Langevin, P., Lafrance, B., Bécu, V., Dubé, B., Kjarsgaard, I., & Guha, J. (2014). The Lemoine auriferous volcanogenic massive sulfide deposit, Chibougamau camp, Abitibi greenstone belt, Quebec, Canada: Geology and genesis. *Economic Geology*, *109*(1), 231–269.

Milkereit, B., & Spencer, C. (1989). Multi-attribute processing techniques for the enhancement and interpretation of seismic data. In *Sixth Multidimensional Signal Processing Workshop,* (p. 40). IEEE.

Milkereit, B., Spencer, C., Agterberg, F. P., & Bonham-Carter, G. F. (1989). Noise suppression and coherency enhancement of seismic data. In *Statistical application in the Earth Sciences* (Vol. 89, pp. 243–248). Geological Survey of Canada.

Mints, M. V. (2017). The composite North American Craton, Superior Province: Deep crustal structure and mantle-plume model of Neoarchaean evolution. *Precambrian Research*, *302*, 94–121.

Moisan, A. (1992). *Pétrochimie des grès de la Formation de Bordeleau, Chibougamau Québec*. Unpublished Master thesis, Université du Québec à Chicoutimi, Chicoutimi, QC, Canada.

Mortensen, J. K. (1993). U–Pb geochronology of the eastern Abitibi subprovince. Part 1: Chibougamau–Matagami–Joutel region. *Canadian Journal of Earth Sciences*, *30*(1), 11–28.

Moyen, J.-F., & Laurent, O. (2017). Archaean tectonic systems: A view from igneous rocks. *Lithos*.

Moyen, J.-F., & Laurent, O. (2018). Archaean tectonic systems: A view from igneous rocks. *Lithos*, *302*, 99–125.

Moyen, J.-F., & Martin, H. (2012). Forty years of TTG research. *Lithos*, *148*, 312–336.

Mueller, W. (1991). Volcanism and related slope to shallow-marine volcaniclastic sedimentation: an Archean example near Chibougamau, Quebec, Canada. *Precambrian Research*, *49*(1–2), 1–22.

Mueller, W., & Donaldson, J. A. (1992). Development of sedimentary basins in the Archean Abitibi belt, Canada: an overview. *Canadian Journal of Earth Sciences*, *29*(10), 2249–2265.

Mueller, W., Chown, E. H., Sharma, K. N. M., Tait, L., & Rocheleau, M. (1989). Paleogeographic and paleotectonic evolution of a basement-controlled Archean supracrustal sequence, Chibougamau-Caopatina, Quebec. *The Journal of Geology*, *97*(4), 399–420.

Naghizadeh, M., Snyder, D., Cheraghi, S., Foster, S., Cilensek, S., Floreani, E., & Mackie, J. (2019). Acquisition and Processing of Wider Bandwidth Seismic Data in Crystalline Crust: Progress with the Metal Earth Project. *Minerals*, *9*(3), 145.

Parman, S. W., & Grove, T. L. (2005). Komatiites in the plume debate. In R. F. Gillian (Ed.), *Plates, plumes, and paradigms* (Vol. 388, p. 249). Boulder, Colo.; Geological Society of America; 1999.

Percival, J. A., & Card, K. D. (1983). Archean crust as revealed in the Kapuskasing uplift, Superior Province, Canada. *Geology*, *11*(6), 323–326.

Percival, J. A., & McGrath, P. H. (1986). Deep crustal structure and tectonic history of the Northern Kapuskasing Uplift of Ontario: An integrated petrological geophysical study. *Tectonics*, *5*(4), 553–572.

Percival, J. A., & West, G. F. (1994). The Kapuskasing uplift: a geological and geophysical synthesis. *Canadian Journal of Earth Sciences*, *31*(7), 1256–1286.

Percival, J. A., Green, A. G., Milkereit, B., Cook, F. A., Geis, W., & West, G. F. (1989). Seismic reflection profiles across deep continental crust exposed in the Kapuskasing uplift structure. *Nature*, *342*(6248), 416.

Petersson, A., Kemp, A. I. S., & Whitehouse, M. J. (2019). A Yilgarn seed to the Pilbara Craton (Australia)? Evidence from inherited zircons. *Geology*, *47*(11), 1098–1102.

Picard, C., & Piboule, M. (1986). Pétrologie des roches volcaniques du sillon de roches vertes archéennes de Matagami-Chibougamau à l'ouest de Chapais (Abitibi est, Québec). 1. Le groupe basal de Roy. *Canadian Journal of Earth Sciences*, *23*(4), 561–578.

Piche, M., Guha, J., & Daigneault, R. (1993). Stratigraphic and structural aspects of the volcanic rocks of the Matagami mining camp, Quebec; implications for the Norita ore deposit. *Economic Geology*, *88*(6), 1542–1558.

Piché, M. (1985). *La formation de Haüy à l'ouest de Chapais; volcanisme sub-aérien en milieu fluviatile*. Unpublished Master thesis, Université du Québec à Chicoutimi, Chicoutimi, QC, Canada.

Pilote, P. (1995). *Metallogenic evolution and geology of the Chibougamau area-from porphyry Cu-Au-Mo to mesothermal lode gold deposits*. Geological Survey of Canada Open File 3143, Québec, Canada.

Pilote, P., Robert, F., Kirkham, R., Daigneault, R., & Sinclair, W. D. (1998). Minéralisation de type porphyrique et filonienne dans le Complexe du lac Doré—le secteur du lac Clark et de l'île Merrill. In Pierre Pilote (Ed.), *Géologie et métallogénie du district minier de Chapais-Chibougamau : Nouvelle vision du potentiel de découverte* (pp. 71–90). MRN report DV 98-03, Ministère des Ressources Naturelles: Québec, QC, Canada.

Pilote, P, Dion, C., Joanisse, A., David, J., Machado, N., Kirkham, R. V, & Robert, F. (1997). Géochronologie des minéralisations d'affiliation magmatique de l'Abitibi, secteurs Chibougamau et de Troilus-Frotet: implications géotectoniques. In *Programme et résumés, Séminaire d'information sur la recherche géologique* (p. 47). MRN report, DV-97-03; Ministère des Ressources Naturelles: Québec, QC, Canada.

Pilote, Pierre. (1986). *Stratigraphie et signification des minéralisations dans le secteur du mont Bourbeau, canton de McKenzie, Chibougamau*. Unpublished Master thesis, Université du Québec à Chicoutimi, Chicoutimi, QC, Canada.

Pitcairn, I. K., & Leventis, N. G. (2017). A metasedimentary source for orogenic gold in the Abitibi belt? In *Mineral Resources to Discover - 14th SGA Biennial Meeting 2017, Volume 1* (pp. 91–94). Society for Geology Applied to Mineral Deposits.

Poitras, A. (1984). *Caractérisation géochimique du Complexe de Cummings, région de Chibougamau-Chapais, Québec*. Unpublished Master thesis, Université du Québec à Chicoutimi, Chicoutimi, QC, Canada.

Potvin, R. (1991). *Étude volcanologique du centre volcanique felsique du Lac des Vents, région de Chibougamau*. Unpublished Master thesis, Université du Québec à Chicoutimi, Chicoutimi, QC, Canada.

Poulsen, K. H. (2017). The Larder Lake-Cadillac break and its gold districts. *Reviews in Economic Geology*, *19*, 133–167.

Racicot, D., Chown, E. H., & Hanel, T. (1984). Plutons of the Chibougamau-Desmaraisville Belt: A Preliminary Survey. In J. Guha & E. Chown (Eds.), *Chibougamau, stratigraphy and mineralization.* (Vol. 34, pp. 178–197). Canadian Institute of Mining and Metallurgy: Westmount, QC, Canada.

Rey, P. F., Philippot, P., & Thébaud, N. (2003). Contribution of mantle plumes, crustal thickening and greenstone blanketing to the 2.75-2.65 Ga global crisis. *Precambrian Research*, *127*(1–3), 43–60.

Ross, P.-S., & Bédard, J. H. (2009). Magmatic affinity of modern and ancient subalkaline volcanic rocks determined from trace-element discriminant diagrams. *Canadian Journal of Earth Sciences*, *46*(11), 823–839.

Rutter, E. H., Khazanehdari, J., Brodie, K. H., Blundell, D. J., & Waltham, D. A. (1999). Synthetic seismic reflection profile through the Ivrea zone-Serie dei Laghi continental crustal section, northwestern Italy. *Geology*, *27*(1), 79–82.

Salisbury, M. H., & Fountain, D. M. (2012). *Exposed cross-sections of the continental crust* (Vol. 317). Springer Science & Business Media.

Schmelzbach, C., Juhlin, C., Carbonell, R., & Simancas, J. F. (2007). Prestack and poststack migration of crooked-line seismic reflection data: a case study from the South Portuguese Zone fold belt, southwestern Iberia. *Geophysics*, *72*(2), B9–B18.

Sénéchal, G., Mareschal, M., Calvert, A. J., Grandjean, G., Hubert, C., & Ludden, J. (1996). Integrated geophysical interpretation of crustal structures in the northern Abitibi belt: constraints from seismic amplitude analysis. *Canadian Journal of Earth Sciences*, *33*(9), 1343–1362.

Sheriff, R. E., & Geldart, L. P. (1995). *Exploration seismology*. Cambridge university press.

SIGEOM. (2020). Système d'information géominière du Québec. Retrieved January 1, 2020, from http://sigeom.mines.gouv.qc.ca

Sizova, E, Gerya, T., Brown, M., & Perchuk, L. L. (2010). Subduction styles in the Precambrian: Insight from numerical experiments. *Lithos*, *116*(3–4), 209–229.

Sizova, Elena, Gerya, T., Stüwe, K., & Brown, M. (2015). Generation of felsic crust in the Archean: a geodynamic modeling perspective. *Precambrian Research*, *271*, 198–224.

Snyder, D. B., Bleeker, W., Reed, L. E., Ayer, J. A., Houle, M. G., & Bateman, R. (2008). Tectonic and metallogenic implications of regional seismic profiles in the Timmins mining camp. *Economic Geology*, *103*(6), 1135–1150.

Stern, R. J. (2005). Evidence from ophiolites, blueschists, and ultrahigh-pressure metamorphic terranes that the modern episode of subduction tectonics began in Neoproterozoic time. *Geology*, *33*(7), 557–560.

Tait, L. (1987). *The character of organic matter and the partitioning of trace and rare earth elements in black shales; Blondaeu Formation, Chibougamau, Québec*. Unpublished Master thesis, Université du Québec à Chicoutimi, Chicoutimi, QC, Canada.

Van Thienen, P., Van den Berg, A. P., & Vlaar, N. J. (2004). Production and recycling of oceanic crust in the early Earth. *Tectonophysics*, *386*(1–2), 41–65.

Trabant, C., Hutko, A. R., Bahavar, M., Karstens, R., Ahern, T., & Aster, R. (2012). Data products at the IRIS DMC: Stepping stones for research and other applications. *Seismological Research Letters*, *83*(5), 846–854.

Watkins, D. H., & Riverin, G. (1982). Geology of the Opemiska copper-gold deposits at Chapais Québec. In R. W. Hutchpor, E. D. Spence, & J. M. Franklin (Eds.), *Precambrian sulphide deposits* (Vol. 25, pp. 427–446). Geological Association of Canada, Mineral Deposits Division: St. John's, NL, Canada.

White, D. J., Musacchio, G., Helmstaedt, H. H., Harrap, R. M., Thurston, P. C., Van der Velden, A., & Hall, K. (2003). Images of a lower-crustal oceanic slab: Direct evidence for tectonic accretion in the Archean western Superior province. *Geology*, *31*(11), 997–1000.

Wörner, G., Mamani, M., & Blum-Oeste, M. (2018). Magmatism in the central Andes. *Elements: An International Magazine of Mineralogy, Geochemistry, and Petrology*,

14(4), 237–244.

Yilmaz, O. (2001). *Seismic data analysis: Processing, inversion, and interpretation of seismic data*. Society of exploration geophysicists. https://doi.org/10.1190/1.9781560801580

Figure 1.

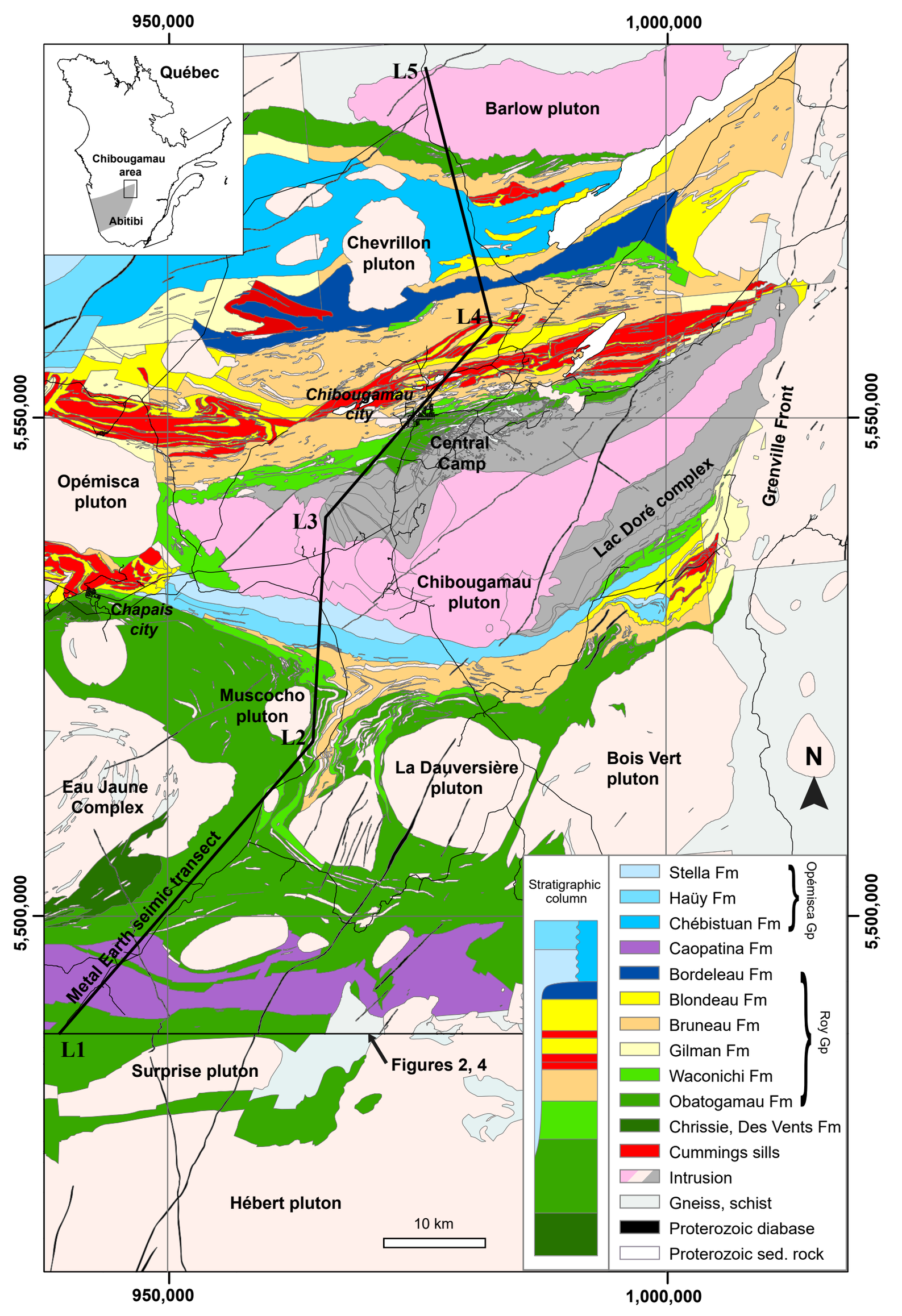
950,000
1,000,000
5,550,000
5,500,000
Québec
Chibougamau area
Abitibi
L5
L4
L3
L2
L1
Barlow pluton
Chevrillon pluton
Chibougamau city
Central Camp
Opémisca pluton
Lac Doré complex
Grenville Front
Chibougamau pluton
Chapais city
Muscocho pluton
Bois Vert pluton
La Dauversière pluton
Eau Jaune Complex
Metal Earth seimic transect
Surprise pluton
Figures 2, 4
Hébert pluton
10 km
N
Stratigraphic column
Stella Fm
Haüy Fm
Chébistuan Fm
Opémisca Gp
Caopatina Fm
Bordeleau Fm
Blondeau Fm
Bruneau Fm
Gilman Fm
Waconichi Fm
Obatogamau Fm
Roy Gp
Chrissie, Des Vents Fm
Cummings sills
Intrusion
Gneiss, schist
Proterozoic diabase
Proterozoic sed. rock

Figure 2.

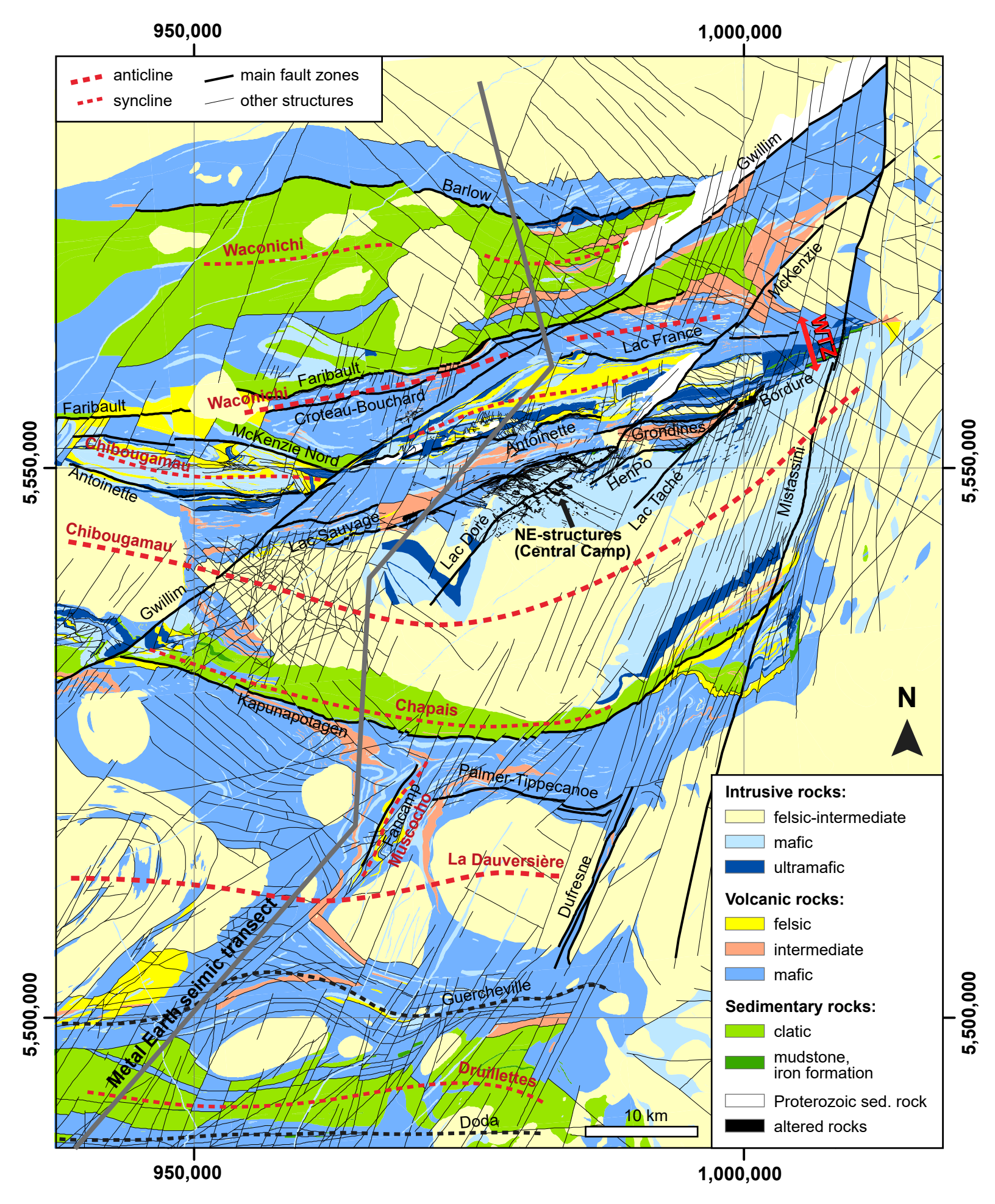
950,000
1,000,000
5,550,000
5,500,000
anticline
syncline
main fault zones
other structures
Barlow
Gwillim
Waconichi
McKenzie
Lac France
MTZ
Faribault
Croteau-Bouchard
Bordure
Chibougamau
McKenzie Nord
Antoinette
Grondines
Hemlo
Lac Taché
Mistassini
Lac Sauvage
Lac Doré
NE-structures
(Central Camp)
Kapunapotagen
Chapais
Palmer-Tippecanoe
Fancamp
Muscocho
La Dauversière
Dufresne
Guercheville
Metal Earth seimic transect
Druillettes
Døda
10 km
N
Intrusive rocks:
felsic-intermediate
mafic
ultramafic
Volcanic rocks:
felsic
intermediate
mafic
Sedimentary rocks:
clatic
mudstone,
iron formation
Proterozoic sed. rock
altered rocks

Figure 3.

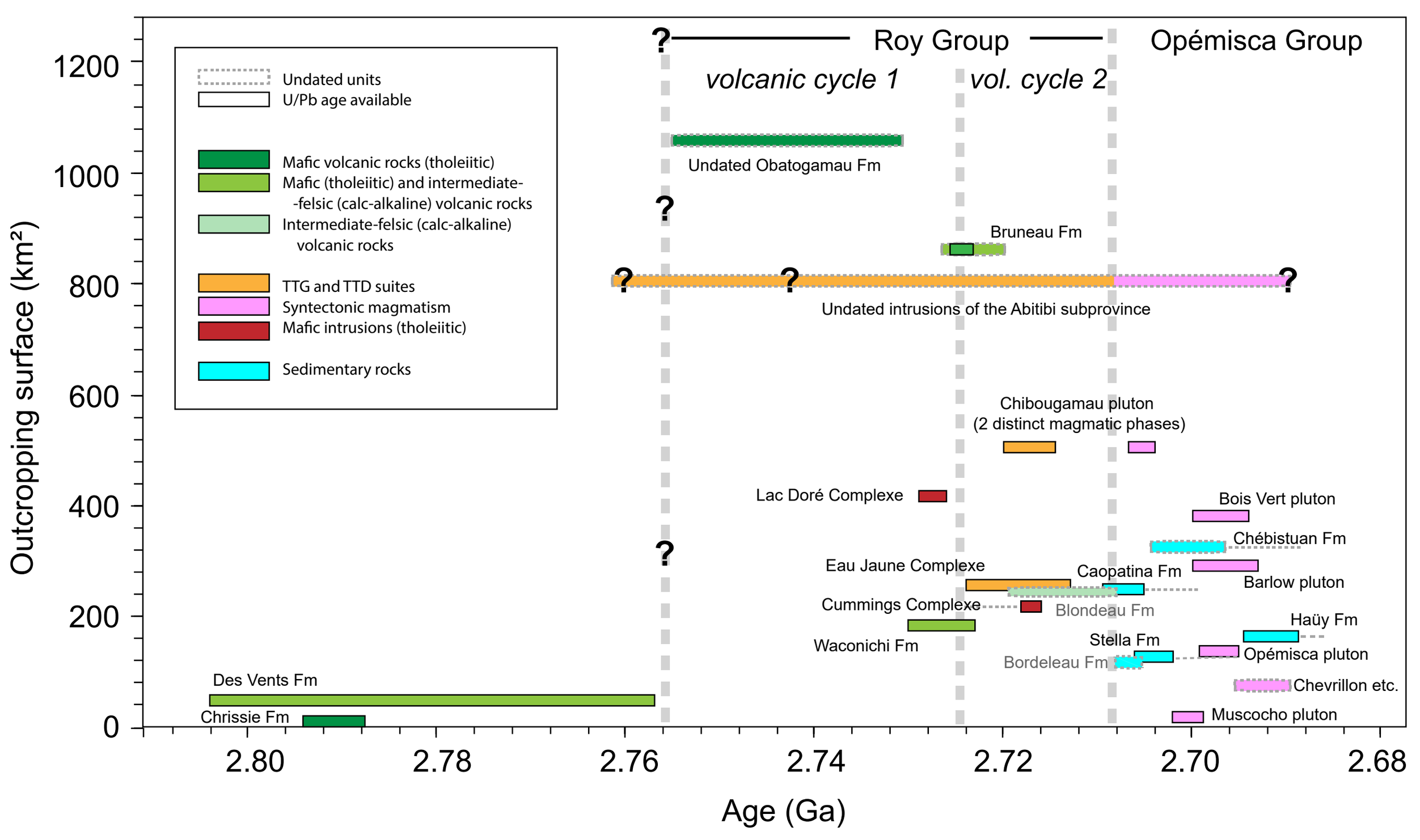
Undated units
U/Pb age available
Mafic volcanic rocks (tholeiitic)
Mafic (tholeiitic) and intermediate--felsic (calc-alkaline) volcanic rocks
Intermediate-felsic (calc-alkaline) volcanic rocks
TTG and TTD suites
Syntectonic magmatism
Mafic intrusions (tholeiitic)
Sedimentary rocks
Roy Group
Opémisca Group
volcanic cycle 1
vol. cycle 2
Undated Obatogamau Fm
Bruneau Fm
Undated intrusions of the Abitibi subprovince
Chibougamau pluton
(2 distinct magmatic phases)
Lac Doré Complexe
Bois Vert pluton
Chébistuan Fm
Eau Jaune Complexe
Caopatina Fm
Barlow pluton
Cummings Complexe
Blondeau Fm
Haüy Fm
Waconichi Fm
Stella Fm
Opémisca pluton
Bordeleau Fm
Chevrillon etc.
Muscocho pluton
Des Vents Fm
Chrissie Fm
Outcropping surface (km²)
Age (Ga)
0
200
400
600
800
1000
1200
2.80
2.78
2.76
2.74
2.72
2.70
2.68

Figure 4.

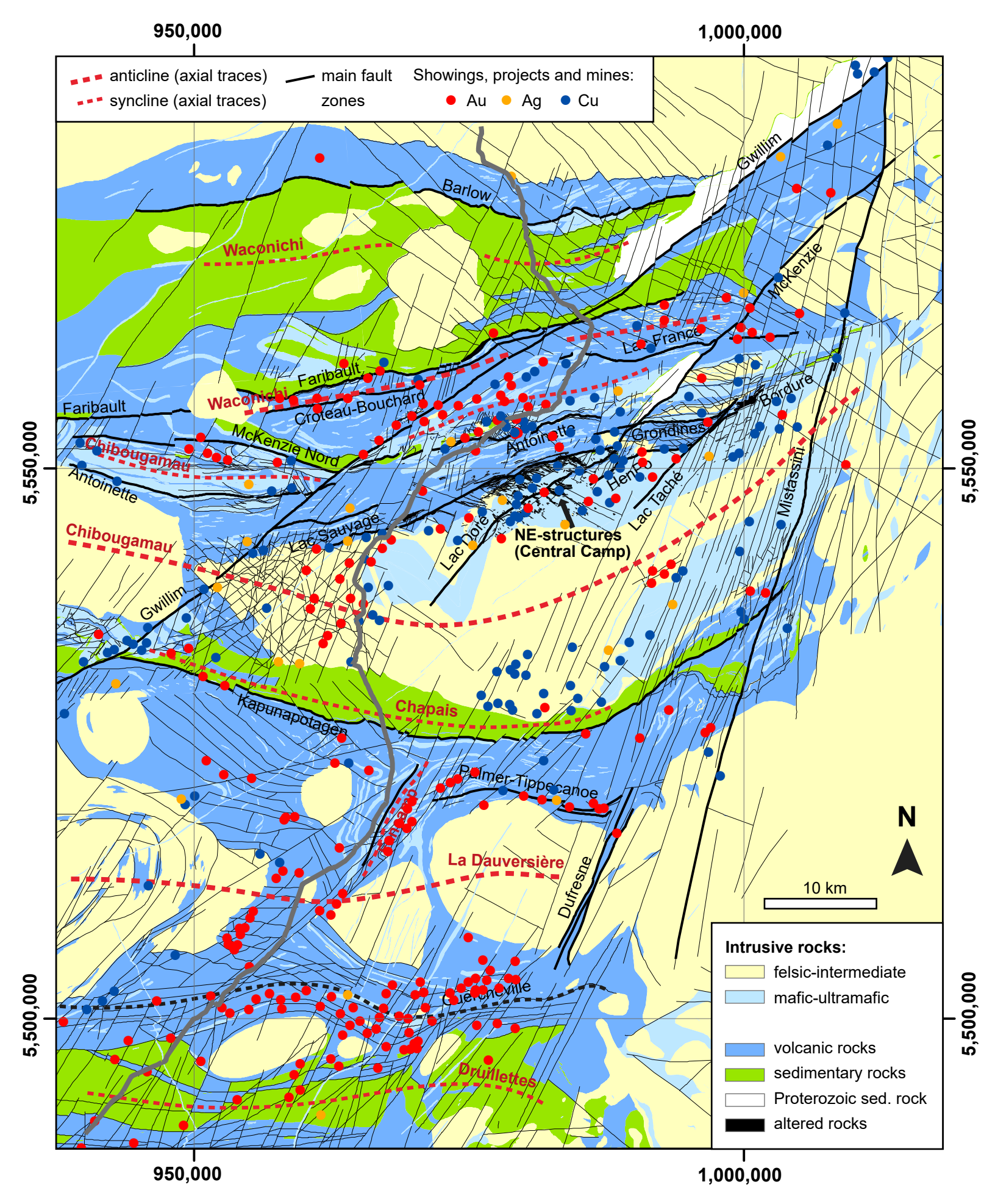
950,000
1,000,000
5,550,000
5,500,000
anticline (axial traces)
syncline (axial traces)
main fault zones
Showings, projects and mines:
Au
Ag
Cu
Barlow
Waconichi
Gwillim
McKenzie
La France
Faribault
Croteau-Bouchard
Bordure
Antoinette
Grondines
Herlig
Lac Taché
Mistassini
Chibougamau
McKenzie Nord
Lac Sauvage
Lac Doré
NE-structures
(Central Camp)
Chapais
Kapunapotagen
Palmer-Tippecanoe
La Dauversière
Dufresne
Guercheville
Druillettes
N
10 km
Intrusive rocks:
felsic-intermediate
mafic-ultramafic
volcanic rocks
sedimentary rocks
Proterozoic sed. rock
altered rocks

Figure 5.

Abitibi Subprovince

Opatica Subprovince

Druillettes

La Dauversière

Chapais

Chibougamau

Chibougamau

Waconichi

Waconichi

Doda FZ

Guercheville FZ

Kapunapotagan FZ

Lac Sauvage FZ

Antoinette FZ

WTZ

Barlow FZ

SSW — NNE

S — N

SSW — NNE

SSE — NNW

CDP

L1

1000

2000

3000

L2

4000

5000

L3

6000

7000

L4

8000

9000

L5

Figure 6a

A

B

B

C

D

Figure 6b

Depth (km)

0

3

6

9

12

15

18

21

24

27

30

33

36

0

10

20

30

40

50

60

70

80

90

100

Distance (km)

Figure 6.

a)

CDP
100
300
500
700
900
1100
1300
1500
1700
1900
Depth (km)
0
3
6
9
12
0
3
6
9
12
15
18
21
Distance (km)

b)

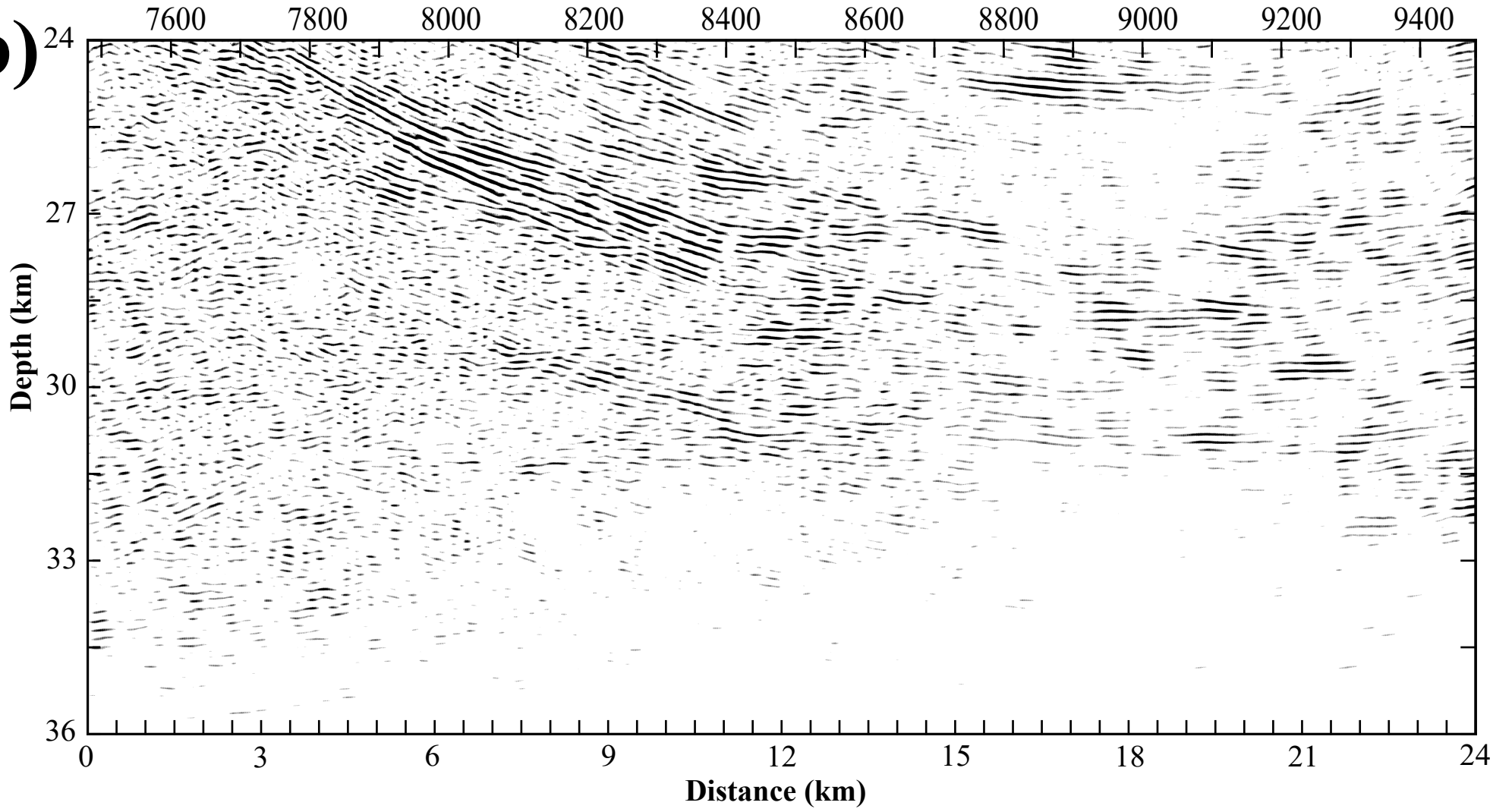
CDP
7600
7800
8000
8200
8400
8600
8800
9000
9200
9400
Depth (km)
24
27
30
33
36
0
3
6
9
12
15
18
21
24
Distance (km)

Figure 7.

a)

SSW — NNE | S — N | SSW — NNE | SSE — NNW

L1 L2 L3 L4 L5 CDP

5a 4 3b 5b 5c 5d 2 1 3 3a 6b 6a

Depth (km)

Distance (km)

1 - 6
Areas described in the text

Reflectors

Moho

Abitibi Subprovince | Opatica Subprovince

Druillettes | La Dauversière | Chapais | Chibougamau | Chibougamau | Waconichi | Waconichi

Doda FZ | Guercheville FZ | Kapunapotagan FZ | Lac Sauvage FZ | Antoinette FZ | WTZ | Barlow FZ

Structures (Figure 2)

Lithologies (Figure 1)

b)

L1 L2 L3 L4 L5 CDP

Upper crust

Mid crust

Lower crust

Opatica

Abitibi

?

?

Depth (km)

Distance (km)

same as Figure 1

Opémisca Group

Intrusions

Mid-crust

Lower crust

Reflectors

Main reflectors

Folds

Contact Abitibi and Opatica subprovinces

Figure 8.

a) **Synvolcanic period (>2.8 - 2.73 Ga)**

Volcanic cycle 1
(central volcano? plateau basalt?)

Lac Doré Complex

More mature crust to the north?
Connected to the Abitibi crust?

Older volcanic rocks

Caopatina Fm?

VMS

S

N

TTG magmatism initiates?

Mafic crust

Nature of lower crust? Mafic cumulats and gneisses? Sialic basement?

b) **Synvolcanic period (2.73 - 2.71 Ga)**

Volcanic cycle 2

?

?

Micro-plates imbircation?
Shortening of continuous crust?

Cu-Au

Shortening
begins?

c) **Syntectonic period (2.71 - 2.69 Ga)**

erosion

erosion

Opémisca Group

Au?

Au?

Main shortening
event?

d) **Syntectonic period (2.69 Ga?)**

Opatica Subprovince

Hébert pluton

Waning stage
of deformation

10 km

Mafic crust, volcanic cycle 1 included (mafic volcanic and intrusive rocks, subordinate felsic volcanism)
Volcanic cycle 2 (mafic and felsic volcanic rocks)
Magmatism (mostly TTG and TTD batholiths, but also mantle-derived magmas)
Magmatism of the syntectonic period (TTG, sanukitoids, alkaline magmatism)
Mid crust region
Lower crust region

Lac Doré Complex
Caopatina Formation (sedimentary rocks)
Opémisca Group (sedimentary rocks)